

The University of Hartford,
College of Engineering, Technology, and Architecture

An Approach to Calculating Live Load Distribution Factors for
Horizontally Curved Bridges with Straight Girders

by

Timothy R. Breiner, B.S.C.E.

Presented to the Faculty of the College of Engineering, Technology, and
Architecture, University of Hartford
As partial requirement for the Degree of Masters of Science

January 2023

NOTE:

The following document has been modified from its original form for upload to timothybreiner.xyz to remove any sensitive information. The written content of the thesis has in no way been modified. For access to the original document, please contact the Harrison Libraries at the University of Hartford.

ABSTRACT

Live load distribution factors (LLDF)s of beam-slab bridges of select typical configurations can be calculated using the approximate equations given by AASHTO BDS 2021. However, these equations are applicable primarily for straight bridges with limited exceptions for curved ones. It is common to use a beam-slab construction with straight prestressed concrete girders in horizontally curved bridges in the United States. For such cases, finite element analysis must be used to calculate LLDFs.

This study developed an approach to calculating LLDFs using generalized finite element tools including geometrical simplifications in models, application of vehicular live load, and data analysis required to calculate the LLDFs. The developed approach was applied to one straight bridge and one curved bridge model, both based on an existing highway bridge in the state of Pennsylvania. Analysis was conducted using two software packages, SAP2000 and CSiBridge, and the LLDFs were calculated for each bridge model from each program. Using these LLDFs, observations were made regarding the accuracy of the loading procedures implemented by each software package and the effects of curvature on the LLDFs for horizontally curved bridges with straight underlying girders.

From the analysis conducted, the following conclusions were made. To calculate accurate LLDFs, CSiBridge is recommended over SAP2000 due to the presence of more features for considering practical distributions of vehicle live load to bridge models. The LLDFs for positive bending moments were impacted more by the effects of horizontal curvature than the LLDFs for negative bending moments. A horizontal curvature causes a greater increase in LLDFs for exterior girders compared to interior girders. Further research was also recommended to validate and expand upon the observations and conclusions made from the results of this study.

Table of Contents

Table of Contents

Table of Figures

Table of Tables

1 Background

1.1 AASHTO BDS Provisions for Vehicular Loading

1.2 AASHTO BDS Provisions for LLDFs

1.3 AASHTO BDS Guidelines for Refined Analysis

1.4 Objectives of Present Study

2 Literature Review

2.1 Chen & Aswad, 1996 – Stretching Span Capability of Prestressed Concrete Bridges Under AASHTO LRFD

2.2 Yousif & Hindi, 2006 – LLDF for Highway Bridges Based on AASHTO LRFD and Finite Element Analysis

2.3 Mensah, 2006 – LLDF in Two-Girder Bridge Systems Using Precast Trapezoidal U-Girders

2.4 Lewis, 2016 – Kinked Straight Girders Forming Horizontally Curved Alignments

2.5 Khalafalla & Sennah, 2014 – Curvature Limitation for Slab-On-I-Girder Bridges

2.6 Zaki, 2016 – LLDFs for Horizontally Curved Concrete Box Girder Bridges

14

- 2.7 Significance of Current Study
- 3 Data Collection and Selection of Bridges
 - 3.1 Data Collection & Database Creation
 - 3.2 Selection of Horizontally Curved Bridge for Analysis
 - 3.2.1 Round One Selection
 - 3.2.2 Round Two Selection
 - 3.3 Detail of the Selected Horizontally Curved Bridge
- 4 Simplification of Finite Element Models
 - 4.1 Simplification of Structural Components and Skew
 - 4.2 Simplification of Horizontally Curved Bridge
- 5 Finite Element Modeling of Bridge Geometry
 - 5.1 Discretization of Elements
 - 5.2 Calculation of Bridge Geometry
 - 5.3 Definition of Element Types
 - 5.4 Finite Element Models
 - 5.5 Verification of Finite Element Modeling Methods
- 6 Live Loading and Calculation of LLDFs
 - 6.1 Load Cases for Horizontally Curved Bridge
 - 6.2 Live Loading Using SAP2000
 - 6.3 Live Loading Using CSiBridge
 - 6.4 Calculation of LLDFs

6.5	Verification of Definition of Live Loads
6.5.1	Detail of Example Bridge
6.5.2	Comparison of Software LLDFs with AAHSTO Hand-Calculated LLDFs 52
6.5.3	Comparison of SAP2000 & CSiBridge LLDFs for Example Bridge
7	Results & Discussion
7.1	Controlling LLDFs
7.1.1	Controlling LLDFs for Horizontally Curved Bridge
7.1.2	Controlling LLDFs for Straight Bridge
7.2	Comparison of LLDFs Calculated with SAP2000 & CSiBridge
7.3	Comparison of Horizontally Curved Bridge & Straight Bridge LLDFs
8	Conclusions & Future Research
	References
9	Appendix

Table of Figures

Figure 1-1: AASHTO HL-93 Design Truck (AASHTO 2012, 3-24)

Figure 1-2: AASHTO HL-93 Design Tandem (CSI 2016, 504)

Figure 3-1: Typical Horizontal Alignment at Road Centerline (Mannering and Washburn 2013, 81)

Figure 3-2: AutoCAD Horizontal Alignment

Figure 3-3: Aerial View of Selected Horizontally Curved Bridge (Google Maps n.d.)

Figure 3-4: Elevation View of Selected Horizontally Curved Bridge (PennDOT 2005, 1)

Figure 3-5: Framing Plan of Selected Horizontally Curved Bridge (PennDOT 2005, 31-33)

Figure 3-6: Transverse Sections of Selected Horizontally Curved Bridge (PennDOT 2005, 2)

Figure 4-1: Simplified Transverse Section of Horizontally Curved Bridge

Figure 4-2: Simplified Framing Plan of Horizontally Curved Bridge

Figure 5-1: Girder Node Position

Figure 5-2: Parabolic Arc

Figure 5-3: Precast Concrete Bulb-Tee Section Input Menu, SAP2000

Figure 5-4: Finite Element Model of Horizontally Curved Bridge

Figure 5-5: Finite Element Model of Straight Bridge

Figure 5-6: Test Bridge

Figure 5-7: Test Bridge Moment Diagrams

Figure 6-1: (a) HL-93K & (b) HL-93S Vehicle Loads in SAP2000 (In Pounds)

Figure 6-2: SAP2000 Finite Element Model of Horizontally Curved Bridge with Lanes

Figure 6-3: SAP2000 Finite Element Model of Straight Bridge with Lanes

Figure 6-4: Moving Load Case Definition - SAP2000

Figure 6-5: Live Load Deformation for (a) Horizontally Curved Bridge & (b) Straight Bridge for All Design Lanes Loaded

Figure 6-6: (Top) HL-93K & (Bot.) HL-93S Vehicle Loads in CSiBridge

Figure 6-7: CSiBridge Finite Element Model of Horizontally Curved Bridge with Lanes

Figure 6-8: CSiBridge Finite Element Model of Straight Bridge with Lanes

Figure 6-9: Moving Load Case Definition - CSiBridge

Figure 6-10: Elevation View of Example Bridge (FHWA 2015, 2-4)

Figure 6-11: Transverse Section of Example Bridge (FHWA 2015, 2-4)

Figure 6-12: Finite Element Model of Example Bridge

Figure 7-1: Positive LLDFs for Horizontally Curved Bridge from SAP2000

Figure 7-2: Negative LLDFs for Horizontally Curved Bridge from SAP2000

Figure 7-3: Positive LLDFs for Horizontally Curved Bridge from CSiBridge

Figure 7-4: Negative LLDFs for Horizontally Curved Bridge from CSiBridge

Figure 7-5: Positive LLDFs for Straight Bridge from SAP2000

Figure 7-6: Negative LLDFs for Straight Bridge from SAP2000

Figure 7-7: Positive LLDFs for Straight Bridge from CSiBridge

Figure 7-8: Negative LLDFs for Straight Bridge from CSiBridge

Table of Tables

Table 1-1: Beam-Slab Deck Cross-Sections with Concrete Supports (AASHTO 2012, 4-33)

Table 1-2: AASHTO LRFD Equations for Moment Distribution Factors in Interior Girders (AASHTO 2012, 4-37)

Table 3-1: Desired Features for Data Collection

Table 3-2: Location of Bridges Selected in Round-One Selection Process

Table 3-3: Degree of Curvature for Five Selected Bridges from Round One Selection Process

Table 3-4: Concrete Strength for Bridge Deck and Girders of Selected Horizontally Curved Bridge

Table 6-1: Live Load Combinations for Horizontally Curved Bridge

Table 6-2: LLDFs of Positive and Negative Bending Moments for the Example Bridge

Table 6-3: Comparison of Software Calculated & Provided LLDFs of Positive and Negative Bending Moments for the Example Bridge

Table 6-4: Comparison of SAP2000 & CSiBridge LLDFs of Positive and Negative Bending Moments for the Example Bridge

Table 7-1: LLDFs of Positive and Negative Bending Moments for the Horizontally Curved Bridge from SAP2000 and CSiBridge

Table 7-2: LLDFs of Positive and Negative Bending Moments for the Straight Bridge from SAP2000 and CSiBridge

Table 7-3: Comparison of SAP2000 & CSiBridge LLDFs for Horizontally Curved Bridge & Straight Bridge

Table 7-4: Comparison of SAP2000 & CSiBridge LLDFs for Horizontally Curved Bridge & Straight Bridge

Table 9-1: LLDFs of Positive and Negative Bending Moments for the Horizontally Curved Bridge from SAP2000

Table 9-2: LLDFs of Positive and Negative Bending Moments for the Straight Bridge from SAP2000

Table 9-3: LLDFs of Positive and Negative Bending Moments for the Horizontally Curved Bridge from CSiBridge

Table 9-4: LLDFs of Positive and Negative Bending Moments for the Straight Bridge from CSiBridge

1 Background

The transfer of vehicular live load from the deck slab of a beam-slab bridge to the underlying support girders may be calculated using live load distribution factors (LLDFs) defined as the percentage of the total vehicle load on the bridge that is transferred to each girder (AASHTO 2012, 4-29). The American Association of State Highway and Transportation Officials (AASHTO) provides guidelines on calculating LLDFs in the AASHTO Load and Resistance Factored Design (LRFD) Bridge Design Specifications (BDS) Article 4.6 (AASHTO 2012, 4-17).

AASHTO BDS provides engineers with approximate equations and guidelines for refined analysis methods to calculate LLDFs for a given bridge. The approximate equations provided by AASHTO are derived from structural analysis and data analysis research and may be easily employed for preliminary design or complex analysis validation by engineers (FHWA 2015, 4-22). Refined analysis methods are those structural analysis methods that satisfy equilibrium and compatibility requirements and incorporate stress-strain relationships (AASHTO 2012, 4-10). While the approximate equations help to simplify the preliminary design process, their applicability is limited to straight bridges with transverse sections matching a select few configurations (AASHTO 2012, 4-33). For bridges with eccentric geometry and/or horizontal curvature, refined analysis is required to calculate the load transfer to the girders. Computerized finite element analysis is used almost exclusively in the modern design process.

1.1 AASHTO BDS Provisions for Vehicular Loading

AASHTO BDS Article 3.6.1 dictates the requirements for vehicular live loading of bridges. To calculate the extreme force effects resulting from vehicle live load, the HL-93 design truck and design tandem loads are applied over one or more design lanes (AASHTO 2012, 3-25). The number of design lanes is specified by AASHTO as the transverse width of the bridge deck divided by 12. To calculate the extreme force effects, the HL-93 loads are then applied over every combination of loaded design lane with the multiple presence factors specified in AASHTO BDS Table 3.6.1.1.2-1.

The HL-93 vehicle load is specified in AASHTO BDS Article 3.6.1.2 as the combination of the HL-93 design truck or design tandem and the design lane load (AASHTO 2012, 3-25). The design truck is presented in Figure 1-1. The design tandem is presented in Figure 1-2.

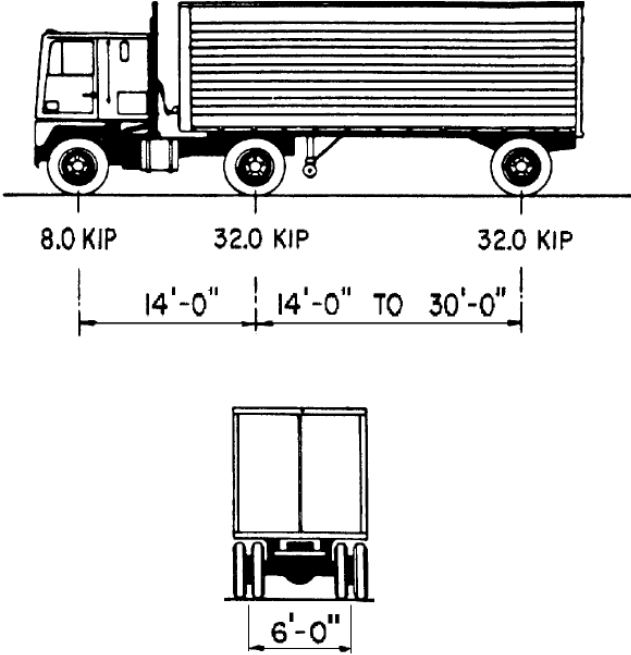


Figure 1-1: AASHTO HL-93 Design Truck (AASHTO 2012, 3-24)

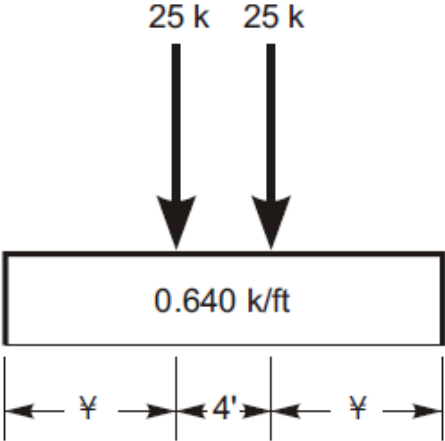


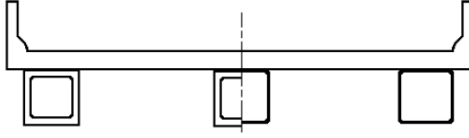
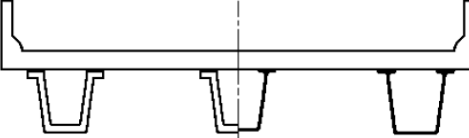
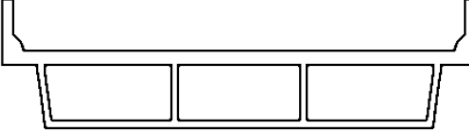
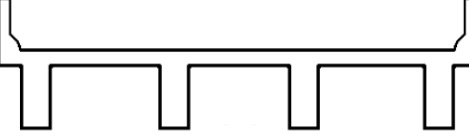
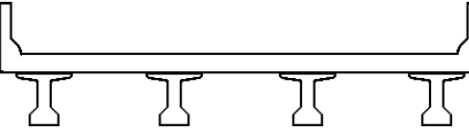
Figure 1-2: AASHTO HL-93 Design Tandem (CSI 2016, 504)

Per AASHTO BDS, the vehicle that produces the more extreme force effect of the design truck and design tandem should be used in analysis. In addition to the concentrated loads at the axles of the design truck and tandem, the HL-93 load includes a 0.64 k/ft linear load that is applied longitudinally over the entire bridge and 10' in the transverse direction (AASHTO 2012, 3-24).

1.2 AASHTO BDS Provisions for LLDFs

The first iterations of the AASHTO approximate equations for calculating LLDFs were applicable for narrow, straight bridges without skew (FHWA 2015, 4-22). With advances in research, the applicability of the approximate equations was expanded to fit varying types of beam-slab bridges. However, the applicability of the equations remains limited by the criteria defined in AASHTO BDS Article 4.6.2.2.1 and the cross-sections defined in AASHTO BDS Table 4.6.2.2.1-1 (AASHTO 2012, 4-33). Select deck superstructure cross-sections defined in AASHTO BDS Table 4.6.2.2.1-1 that are supported by concrete components are presented in Table 1-1.

Table 1-1: Beam-Slab Deck Cross-Sections with Concrete Supports (AASHTO 2012, 4-33)

Type of Deck	Supporting Components	Typical Cross-Section
Cast-in-Place Concrete Slab	Precast Concrete Boxes/Closed Steel Boxes	
Cast-in-Place or Precast Concrete Deck Slab	Precast Concrete Boxes/Open Steel	
Monolithic Concrete	Cast-in-Place Concrete Multicell Box	
Monolithic Concrete	Cast-in-Place Concrete Tee Beam	
Cast-in-Place or Precast Concrete Deck Slab	Precast Concrete I or Bulb-Tee Sections	

AASHTO BDS Article 4.6.2.2 defines the procedures for calculating LLDFs using the approximate equations derived from statistical data and the Lever Rule (Mensah 2006, 7). To apply these procedures, the bridge that is being analyzed must meet the criteria defined in Article 4.6.2.2.1 (AASHTO 2012, 4-29):

- Width of the deck must be constant.
- The number of beams may not be less than four unless otherwise specified.
- Beams must have approximately the same stiffness and must run parallel.
- Overhang that includes the roadway must not exceed 3' unless otherwise specified.

- For curved bridges, curvature in plan must be less than the limits established in Article 4.6.1.2.4. This restriction may be bypassed in cases where distribution factors are deemed necessary to implement an analysis method that would satisfy the structural analysis requirements of Article 4.4.
- Cross-sections must be consistent with those shown in Table 4.6.2.2.1-1.

If the above criteria are not met, refined analysis methods (AASHTO BDS Article 4.6.3) are required to calculate the LLDFs.

The equations to calculate LLDFs for the cross-sections defined in Table 1-1 are tabulated in AASHTO BDS for exterior girders and interior girders. AASHTO BDS Tables 4.6.2.2.2b-1 & 4.6.2.2.d-1 provides the equations to calculate the LLDFs for interior girders and exterior girders respectively. Table 1-2 presents a portion of AASHTO BDS Table 4.6.2.2.2b-1 for calculating the interior girder LLDFs. AASHTO BDS may be referenced for the full version of the above referenced tables.

Table 1-2: AASHTO LFRD Equations for Moment Distribution Factors in Interior Girders (AASHTO 2012, 4-37)

Type of Superstructure	Applicable Cross-Section from Table 4.6.2.2.1-1	Distribution Factors	Range of Applicability
Concrete Deck, Filled Grid, Partially Filled Grid, or Unfilled Grid Deck Composite with Reinforced Concrete Slab on Steel or Concrete Beams; Concrete T-Beams, T- and Double T-Sections	a, e, k and also i, j if sufficiently connected to act as a unit	One Design Lane Loaded: $0.06 + \left(\frac{S}{14}\right)^{0.4} \left(\frac{S}{L}\right)^{0.3} \left(\frac{K_g}{12.0Lt_s^3}\right)^{0.1}$	$3.5 \leq S \leq 16.0$ $4.5 \leq t_s \leq 12.0$ $20 \leq L \leq 240$ $N_b \geq 4$ $10,000 \leq K_g \leq 7,000,000$
		Two or More Design Lanes Loaded: $0.075 + \left(\frac{S}{9.5}\right)^{0.6} \left(\frac{S}{L}\right)^{0.2} \left(\frac{K_g}{12.0Lt_s^3}\right)^{0.1}$	
		use lesser of the values obtained from the equation above with $N_b = 3$ or the lever rule	
Cast-in-Place Concrete Multicell Box	d	One Design Lane Loaded: $\left(1.75 + \frac{S}{3.6}\right) \left(\frac{1}{L}\right)^{0.35} \left(\frac{1}{N_c}\right)^{0.45}$ Two or More Design Lanes Loaded: $\left(\frac{13}{N_c}\right)^{0.3} \left(\frac{S}{5.8}\right) \left(\frac{1}{L}\right)^{0.25}$	$7.0 \leq S \leq 13.0$ $60 \leq L \leq 240$ $N_c \geq 3$ If $N_c > 8$ use $N_c = 8$
Concrete Deck on Concrete Spread Box Beams	b, c	One Design Lane Loaded: $\left(\frac{S}{3.0}\right)^{0.35} \left(\frac{Sd}{12.0L^2}\right)^{0.25}$ Two or More Design Lanes Loaded: $\left(\frac{S}{6.3}\right)^{0.6} \left(\frac{Sd}{12.0L^2}\right)^{0.125}$	$6.0 \leq S \leq 18.0$ $20 \leq L \leq 140$ $18 \leq d \leq 65$ $N_b \geq 3$
		Use Lever Rule	$S > 18.0$

Per the criteria defined in AASHTO BDS Article 4.6.2.2.1, the applicability of the approximate equations is limited for horizontally curved bridges. Article 4.6.1 sets curvature in plan limits for which horizontally curved bridges with curved supporting girders may be analyzed as straight segments (AASHTO 2012, 4-17). For curved bridges with concrete girders, limits are set for only concrete box girder bridges. For bridges not meeting these limitations, refined analysis methods are required to calculate LLDFs.

The curvature limitations set in AASHTO BDS Article 4.6.1.2.3 for concrete box girder bridges consider horizontally curved bridges with straight segmented box girders and nonsegmental curved box girders. Horizontally curved concrete box girders with straight segments bridges may be designed for central angles 12° or less within one span (AASHTO 2012, 4-19). Nonsegmental curved box girders may be designed for global force effects as single-spine beams with straight segments for central angles of 34° or less within one span. For segmented curved box girder superstructures with central angles within one span between 12° and 34° , analysis may be conducted as a single-spine beam with straight segments so long as no segment has a central angle exceeding 3.5° . If these limitations are exceeded, AASHTO BDS requires that analysis shall be conducted using a proven 3D analysis method with six degrees of freedom (AASHTO 2012, 4-20).

1.3 AASHTO BDS Guidelines for Refined Analysis

AASHTO BDS Article 4.6.3 provides guidelines for using refined analysis methods to calculate LLDFs for beam-slab bridges. Per the specifications, an acceptable method of structural analysis is “any method of analysis that satisfies the requirements of equilibrium and compatibility and utilizes stress-strain relationships for the proposed materials” (AASHTO 2012, 4-9 - 4-10). Of the examples that are listed as acceptable methods, the most prominent method is finite element analysis. This method is preferred due to its relative simplicity in comparison to classical analysis methods.

AASHTO BDS Article 4.6.3.2 provides guidelines for the finite element modeling of a bridge deck. For deformation analysis, flexural and torsional deformation shall be considered while vertical shear deformation may be neglected (AASHTO 2012, 4-69). For modeling an

orthotropic deck slab, three-dimensional finite shell elements or solid elements are recommended, and all components shall be included in the model.

AASHTO BDS Article 4.6.3.3 provides guidelines for the aspect ratio of elements when modeling a beam-slab bridge. Per the specifications, the ratio of finite elements/grid panels shall not exceed 5.0 and abrupt changes in element geometry are not advised (AASHTO 2012, 4-70). Provided in the specifications is a commentary section with additional guidelines for modeling. Per this commentary, five to nine grid nodes per beam span is recommended. For bridges modeled with shell and beam elements, it is recommended that the relative elevation differences be maintained.

1.4 Objectives of Present Study

The approximate equations provided by AASHTO BDS for calculating LLDFs are limited in their applicability to horizontally curved bridges. For bridges with curvature exceeding the limits set in Article 4.6.1, refined analysis is required to analyze and design the underlying bridge girders (AASHTO 2012, 4-17). Therefore, most curved bridges that are supported by concrete girders require the use of finite element analysis.

The focus of this study was the calculation of LLDFs for horizontally curved bridges supported by straight underlying concrete girders using the finite element software packages SAP2000 and CSiBridge. In the United States, construction of horizontally curved bridges with straight underlying precast concrete I-girders is preferred over curved precast concrete I-girders due to complexity in fabrication and transportation (Amorn, Tuan and Tadros 2008, 48). As previously stated, the eccentric geometry of these types of bridges do not allow the approximate equations from AASHTO BDS to be used. Therefore, finite element analysis is used by engineers in all steps of the design to calculate the load transfers from the deck to the girders.

The software packages used for geometric finite element modeling and vehicular loading and analysis of the bridges were SAP2000 and CSiBridge by Computers & Structures, Inc. (CSI 2016). SAP2000 is a generalized software package that may be used to model and analyze structures with complex geometry. CSiBridge is a companion software package to SAP2000 that is optimized for detailed vehicle loading and load rating of bridges. While CSiBridge is

recommended by the manufacturers for vehicular loading of bridges, moving load functionality is present in the SAP2000 software package (CSI 2016, 477).

This study developed an approach to calculating LLDFs for horizontally curved bridges with underlying straight girders using generalized finite element tools including geometrical simplifications in models, application of vehicular live load, and data analysis required to calculate the LLDFs. To model the complex geometry of the bridges, SAP2000 was preferred over CSiBridge due to the presence of interactive spreadsheet inputs and the generalized structural modeling tools available in SAP2000 (CSI 2016, 2). Vehicular live loading was conducted using both SAP2000 and CSiBridge to investigate the differences between the two software packages and its effect on the structural response of the bridge models.

The developed finite element modeling and loading approach was verified using an example bridge designed by the FHWA with existing LLDF calculations per AASHTO BDS (FHWA 2015, 5-9). This modeling approach was then applied to one straight bridge and one curved bridge model, both based on an existing highway bridge in the state of Pennsylvania. Using the LLDFs calculated from SAP2000 and CSiBridge for these models, observations were made regarding the accuracy of the loading procedures implemented by each software package and the effects of curvature on the LLDFs for horizontally curved bridges with straight underlying girders.

2 Literature Review

A review of existing literature related to the topic of study was conducted. This literature review was conducted to better understand the following: application of the AASHTO specifications, finite element modeling techniques, observed structural behavior of underlying bridge girders, data analysis methods, and limitations of the AASTO LLDF equations. Studies, technical reports, and design reports were reviewed that pertained to the previously stated research goals. The literature that was reviewed included fundamental studies whose results were incorporated into the AASHTO specifications, studies that verified the accuracy of the AASHTO LLDF equations, and studies that investigated bridge types and configurations where the AASHTO equations were not applicable.

2.1 Chen & Aswad, 1996 – Stretching Span Capability of Prestressed Concrete Bridges Under AASHTO LRFD

This study was conducted to verify the accuracy of the 1994 AASHTO BDS equations for calculating LLDFs for prestressed concrete bridges constructed with I-girders or spread box girders with large span to depth ratios. The 1994 LRFD approximate analysis simplified equations were derived using a set of average bridges which, for I-beam superstructures, had smaller spans than a I-girder bridge superstructure (Chen and Aswad 1996, 112). Additional concerns regarding these equations were raised regarding their overconservative nature as well as the rejection of multilane reduction factors in development. The accuracy of the 1994 equations were verified for the mentioned configurations by comparing LLDFs calculated using finite element analysis to those calculated with the simplified equations.

Finite element modeling following the 1994 AASHTO BDS refined analysis recommendations was conducted for the I-girder and spread box beam bridges. The bridge deck was modeled using both shell and beam elements and was modeled separately from the underlying girders, allowing for different material properties to be used (Chen and Aswad 1996, 114). Additional conditions and assumptions were applied to the models. These conditions simplified the model by assuming

linear elastic behavior and by not considering extraneous forces and bending that would not significantly contribute to the load distribution factors.

The LLDFs obtained from the finite element analysis and approximate LRFD equations were compared. It was found that, for both girder configurations, the LLDFs calculated using the approximate equations were significantly more conservative than those calculated by finite element analysis. Based on these findings, it was recommended by the authors that refined analysis be used to calculate LLDFs for prestressed concrete bridges with long spans (Chen and Aswad 1996, 120). Compared to the 1994 AASHTO BDS equations, refined analysis allowed for significant release strength reduction for the girder system.

2.2 Yousif & Hindi, 2006 – LLDF for Highway Bridges Based on AASHTO LRFD and Finite Element Analysis

This study was conducted in response to significant changes made in the 2004 AASHTO BDS in relation to LLDF calculation procedures. In comparison to the 1996 AASHTO specifications, the 2004 specifications introduced additional parameters and limitations that would result in more accurate LLDF values (Yousif and Hindi 2006, 2). Prior research conducted during the study concluded that the 2004 AASHTO BDS methods are less conservative than the 1996 AASHTO methods, but still conservative compared to refined analysis methods. To verify that the 2004 AASHTO LRFD LLDF methods will result in safe highway bridges, LLDFs calculated in accordance with the AASHTO specifications were compared with those obtained by finite element analysis for concrete bridges that covered the range of applicability specified by AASHTO.

The study evaluated four finite element modeling techniques and selected the technique that was believed to be the most accurate and practical (Yousif and Hindi 2006, 7). The selected modeling technique idealized the bridge as a two-dimensional system with the following procedures (Yousif and Hindi 2006, 7).

- The main girders and ends diaphragm beams were modeled as space frame elements with six degrees of freedom (DOFs) at each node.
- The properties of the girders were transformed to the deck's center of gravity.

- Girders were simply supported with hinge and roller supports at opposite ends.
- Per AASHTO LRFD recommendations on torsional restraint, full depth diaphragm was provided at each support.
- A shell length to width aspect ratio of 1.02 was provided which is within the AASHTO LRFD specification of acceptable aspect ratios, ≤ 5 .

This modeling procedure was selected by cross-referencing the results of a benchmark bridge with two prior studies (Yousif and Hindi 2006, 8).

The results of the finite element analysis and hand calculations were compared (Yousif and Hindi 2006, 10). The LLDFs calculated by hand using the AASHTO equations were found to be conservative. For one lane loaded, the AASHTO LLDFs became less conservative for exterior girders as longitudinal stiffness increased. For interior girders, short span lengths with large longitudinal stiffness caused the AASHTO LLDFs to become less conservative. For two lanes loaded, the AASHTO LLDFs became less conservative for exterior girders as the span length was increased. The same effect was noticed for exterior girders subjected to three lanes loaded. For interior girders subjected to two lanes loaded, the AASHTO LLDFs became more conservative as the span length increased. The study concluded that the AASHTO equations are adequate for bridges subjected to one or two lanes loaded (Yousif and Hindi 2006, 10). For bridges subjected to three or more lanes loaded, finite element analysis was recommended.

2.3 Mensah, 2006 – LLDF in Two-Girder Bridge Systems Using Precast Trapezoidal U-Girders

This study was conducted in response to economic concerns raised about the degree of conservatism present in the Lever Rule method of LLDF calculation outlined in AASHTO BDS. Two-girder bridge systems with precast trapezoidal girders were selected as the focus of the study due to the increasing use of the design and its adoption by the Colorado Department of Transportation (Mensah 2006, 1). Since the Lever Rule method is used to design these types of bridge superstructures, concerns that bridges were being built that were too expensive were raised.. To address these concerns, the Lever Rule methods were compared to refined methods to

determine how accurately the Lever Rule method reflects the real response of two-girder bridges with precast trapezoidal girders.

Finite element modeling was conducted using the eccentric beam method, a popular method for modeling bridges that accounts for the composite action between the centers of the bridge deck and the underlying girders (Mensah 2006, 26). Using this modeling technique, the bridge slab was idealized as four-node shell elements and the underlying girders were idealized as two-node iso-parametric beam elements (Mensah 2006, 50). Rigid link elements were used to connect the slab and beam elements at the object centroids, representing the composite action of the structural members. An experimental bridge was analyzed and compared with live load data from a previous study to validate this technique.

Crack control considerations were made before analysis was conducted. When a concrete section is cracked it becomes ineffective in tension, resulting in a less rigid transverse section. Increased flexibility in the deck results in worse load distribution, therefore resulting in higher LLDFs (Mensah 2006, 67). For this reason, two-girder bridges are typically sized using gross sectional properties to prevent deck slab cracking.

For the bridges that were investigated, the Lever Rule method generated LLDFs that were 25% more conservative than those calculated using finite element analysis (Mensah 2006, 105). Reduction of strands, girder depth, and an increase in span length was investigated to determine if cost cutting measures could be made and still fall within acceptable safety parameters. It was found that significant reductions to the number of strands and girder depth and a significant increase in span length can be made if finite element methods are employed (Mensah 2006, 106).

2.4 Lewis, 2016 – Kinked Straight Girders Forming Horizontally Curved Alignments

This report was written to detail the use of kinked straight girders supporting horizontally curved beam-slab bridges in Edmonton, Alberta, Canada. Design considerations in accordance with Canadian federal code and Alberta province code were detailed along with references to AASHTO BDS. The multi-span bridges highlighted in the report were designed with straight plate I-girders with kinks that formed a segmentally curved line at the request of the contractor

(Lewis 2016, 2). Per AASHTO BDS, continuously kinked girders may be treated as horizontally curved girders. However, due to concentrated force effects that occur at the girder kinks, additional considerations must be accounted for.

In a curved girder system, flange loads act as distributed out of plane loads (Lewis 2016, 3). In a kinked girder system, a concentrated load is generated at the kink, resulting in lateral bending of the flange. Since straight flanges are not subject to bowing in compression or straightening under tension (both occur in curved girder flanges), straight girder equations were used to calculate the kinked girder capacity. In the web, tension field action was neglected at the discrete bends in the web alignment (Lewis 2016, 3).

Finite element modeling using 3D plate eccentric beam models was used for the kinked girder system with special considerations regarding flange lateral bending and non-composite deflections (Lewis 2016, 3). The modeling software used neglected the contribution of flange lateral bending which caused unexpected non-composite deflections to be reported. A revised model using frame elements for the flanges and shell elements for the web was employed that resulted in a smoother, less disjointed model. The analysis results from the revised model reported a 30% deflection decrease from the original model (Lewis 2016, 7).

2.5 Khalafalla & Sennah, 2014 – Curvature Limitation for Slab-On-I-Girder Bridges

This study was conducted to investigate the AASHTO specifications for treatment of horizontally curved steel and concrete slab-on-I-girder bridges. The AASHTO specifications allow for curvature effects to be neglected for steel I-girders based on the central angle (Khalafalla and Sennah 2014, 1). Curvature limitations for concrete I-girders are not provided. A total of 126 concrete I-girder bridges were analyzed under dead load using finite element methods to investigate the behavior of curvature effects and to compare with the AASHTO specifications (Khalafalla and Sennah 2014, 2). A series of equations to limit curvature neglect was developed to improve the accuracy of the AASHTO specifications.

Bridge analysis was conducted using specified assumptions and modeling techniques. Bridges were assumed to have elastic and homogenous materials, no skew lines, and no force effects

coming from road superelevation and curbs (Khakafalla and Sennah 2014, 4). The concrete deck slab, girders, and diaphragms were modeled using a four-node shell element with six DOFs at each node. The concrete deck slabs between webs in cross sections were modeled using four shell elements in the horizontal direction. For the deck cantilever, two horizontal shell elements were used.

A parametric study was conducted with the data generated by the finite element analysis to evaluate the magnification of selected factors for curved bridges in comparison to straight bridges of similar geometry (Khakafalla and Sennah 2014, 6). The key parameters that influenced curved bridge structural response were found to be the span to curvature radius ratio (L/R), bridge span length (L), bridge width (B), and continuity.

The authors found that curvature was the principal factor that influences structural behavior of horizontally curved bridges (Khakafalla and Sennah 2014, 13). Increases in curvature increase maximum flexural stress, vertical deflection, and support reactions. It was found that the AASHTO procedures greatly underestimated responses in curved bridges that the specifications would allow to be treated as straight bridges. The authors proposed a set of equations limiting curvature based on key structural parameters to Code writers.

2.6 Zaki, 2016 – LLDFs for Horizontally Curved Concrete Box Girder Bridges

This study was conducted to address the central angle limitations imposed by the AASHTO LLDF equations on horizontally curved bridges with underlying concrete box girders. For bridges with a central angle exceeding 34° , AASHTO BDS states that refined analysis is necessary (AASHTO 2012, 4-20). The LLDFs for horizontally curved concrete box girder bridges with central angles exceeding 34° at one span were calculated using finite element analysis and hand calculations with the AASHTO BDS approximate equations (Zaki 2016, 5).

Horizontally curved concrete box girder bridges based on real geometry were analyzed with varying span lengths and varying central angles (Zaki 2016, 19). Additionally, straight bridges using the specified span lengths were analyzed to conceptualize the degree of conservatism of the AASHTO equations. The LLDFs for the horizontally curved bridges were compared using

the straight bridge LLDFs as a control for each central angle variation. Additional analysis was conducted for the horizontally curved bridges accounting for centrifugal and braking force effects.

CSiBridge was used for the finite element modeling and analysis of the bridges. Shell elements were used to model the bridge deck slab, box girders, and substructure per recommendations from CSI and prior research (Zaki 2016, 21-22). Rigid link elements were used to connect the bridge superstructure to the substructure elements.

For a straight bridge with concrete box girders, it was concluded that the AASHTO equations were conservative (Zaki 2016, 71). The equations provided more conservative results for the exterior girders than the interior girders. It was also noted that the AASHTO LLDFs became less conservative as the span length was increased.

For a horizontally curved bridge with concrete girders, the following conclusions were made. For a span within the same central angle, the LLDFs decreases as the span length increases (Zaki 2016, 71-72). The LLDF increases with increasing box girder curvature. LLDFs for bridges with a small degree of curvature ($\leq 5^\circ$) are not significantly different than those for straight bridges. The AASHTO equations for LLDFs are applicable for curved concrete box girder bridges with curvature slightly larger than 34° , possible up to 38° . The application of centrifugal and braking force effects resulted in a significant increase in maximum moment for exterior girders and a general increase in bending moment for all girders due to braking forces.

2.7 Significance of Current Study

The findings of the literature review were applied to develop methodologies for finite element analysis and data analysis. It was found that, while different software packages were used, similar modeling techniques were employed by the various researchers. The eccentric beam method was commonly used to connect the bridge deck and underlying girder elements together (Mensah 2006, 26). As per the recommendations from AASHTO, shell elements were used by all the researchers to model the bridge deck slab. The types of elements used to model the underlying girders was largely dependent on the type of girder being modeled. For concrete I-

beam bridges, beam elements were the most used type of element for finite element modeling of the girders (Chen and Aswad 1996, 113).

Several studies compared finite element techniques to the AASHTO approximate equations. From these studies, common conclusions were drawn. Within the ranges of applicability, the AASHTO equations produce conservative LLDFs compared to finite element analysis (Zaki 2016, 71). The equations produce less conservative LLDFs when the longitudinal stiffness and span length are increased (Yousif and Hindi 2006, 10) (Zaki 2016, 71-72). When curvature is introduced, the AASHTO equations become unreliable since complex force effects are introduced but are not considered in the equations (Lewis 2016, 3-5) (Zaki 2016, 71-72) (Khakafalla and Sennah 2014, 13). However, the extent of research discussing the impact of curvature on LLDFs is limited.

The findings of the literature review proved the necessity of the project goals. The existing research on the effects of curvature on LLDFs is limited. Design considerations for horizontally curved bridges with straight underlying girders are not adequately covered by the existing research. The procedures employed by researchers for finite element analysis are often understated. Outside of the AASHTO specifications for finite element analysis, supplemental guidelines and simplifications for modeling and detailed design examples are difficult to find.

Additionally, there is no existing research comparing the moving load capabilities of SAP2000 and CSiBridge software packages. While it is known that CSiBridge provides more detailed bridge analysis tools, SAP2000 also provides moving load tools that may be used for vehicular loading of bridge models (CSI 2016, 479-480). For engineers and researchers that do not have access to the CSiBridge software package, understanding the capabilities of each software package and the degree of error to be expected when using one over the other is of vital importance to their work.

3 Data Collection and Selection of Bridges

Data was collected on existing curved highway bridges with straight underlying concrete girders. Requests for information regarding existing bridges were sent to state DOTs in the northeastern United States. From these requests, construction drawings for 17 bridges located in the states of Virginia, Vermont, and Pennsylvania were obtained.

Data for the 17 bridges were cataloged into a database to highlight bridge parameters relevant to the project. A two-round selection process was conducted to select one horizontally curved bridge with straight underlying girders that would be modeled using the developed finite element modeling approach.

3.1 Data Collection & Database Creation

Before research was done to find existing bridge superstructure data, desired features were established to guide the research process. These features established the basic geometric properties, material properties, governing Code, and desired format of the data that was to be collected. The desired features are presented in [Table 3-3](#).

Table 3-3: Desired Features for Data Collection

Type	
Geometry	Horizontally curved span Straight underlying girders
Materials and Structural Type	Concrete cast-in-place deck Prestressed concrete underlying girders
Design Codes	AASHTO Bridge Design Specifications (any year)
Data Format	Construction/As-Built Drawings Construction Specifications Finite Element Models Structural Analysis/Design Calculations

With the research parameters considered, requests for data were sent to State Departments of Transportation (DOTs) in the northeast United States. Construction drawings were received from the states of Virginia, Vermont, and Pennsylvania for a total of 17 bridges. In addition to the drawings provided by the state DOTs, supplemental bridge data from the U.S. Federal Highway Administration's (FHWA) National Bridge Inventory (NBI) were obtained for each bridge.

The bridges for which bridge data were provided by the state DOTs conformed to the parameters defined in **Table 3-3**. All the bridges were horizontally curved with a concrete deck and straight prestressed concrete girders. Depending on the age of the bridge, either the Standard or LRFD versions of AASHTO BDS was the governing code for the bridge design. For all bridges, construction drawings or as-built drawings were provided.

To compare the geometric and material properties of the bridges, a spreadsheet database was created. For each bridge, the location of the bridge, geometric properties, material properties, design codes followed, and specified bridge loads were catalogued. Using the database, trends in the bridge properties were observed. Cast-in-place concrete with a 28-day compressive strength of 4000 psi was used as the concrete type in the deck most frequently (PennDOT 2019, 106). The average minimum bridge deck thickness was 8.30 in. The predominant girder cross-sections were bulb-tee/concrete I-sections.

3.2 Selection of Horizontally Curved Bridge for Analysis

A two-round selection process was employed to select the bridge that would be modeled and analyzed using the developed finite element approach. Selection criteria were considered to select a bridge with a large degree of curvature so that the effects of curvature on LLDFs may be observed. Additionally, criteria were considered to eliminate bridges with drawings that did not provide adequate information for finite element modeling and bridges where the provided drawings could not be easily read due to poor scan quality.

3.2.1 Round One Selection

The first round of the selection process limited the full pool of 17 bridges to five bridges. Since all bridges matched the desired configuration, horizontally curved bridge deck with straight prestressed concrete underlying girders, elimination based on these criteria were not necessary. Instead, selection was conducted to eliminate all but five bridges based on the level of detail and legibility of the provided construction drawings for each bridge.

To select five bridges, a list of desired criteria was created. These criteria were written to select bridges that would be easy to model and produce accurate analysis results. The list of desired criteria for the first-round selection is listed below in order of importance.

1. Legibility/visual fidelity of the scanned drawings.
2. Established reference coordinates either through a stake-out plan or some other means.

Since creating an accurate finite element model of the bridges would require close attention to detail, legibility was deemed the most critical criterion. Any set of drawings that could not be read (primarily due to bad scan quality) were immediately discarded without considering any of the other criteria. The presence of reference coordinates in the drawing sets was desired so that the curvature of the bridge deck and angle of the bridge piers and abutments could be accurately calculated and modeled.

Using the selection criteria, five bridges were selected from the original pool of data. These bridges were all located in Pennsylvania by coincidence. The location of the five bridges that passed the first-round selection process are presented in **Table 3-4**.

Table 3-4: Location of Bridges Selected in Round-One Selection Process

Latitude (Dec. Degrees)	Longitude (Dec. Degrees)	Road Carried
41.82359	-77.08797	PA State Road 15
39.82127	-79.04704	PA State Road 6219 NB
41.99702	-77.13819	PA State Road 15 SB
41.99718	-77.13776	PA State Road 15 NB
40.23202	-77.87383	PA State Road 0522 Sec. 5BS

3.2.2 Round Two Selection

A second and final elimination was conducted to choose the bridge with the largest degree of curvature of the five bridges selected in the first round. To calculate the degree of curvature of each bridge, the road centerline was used to create a horizontal alignment (Mannering and Washburn 2013, 77-91). A typical horizontal alignment is presented in [Figure 3-3](#).

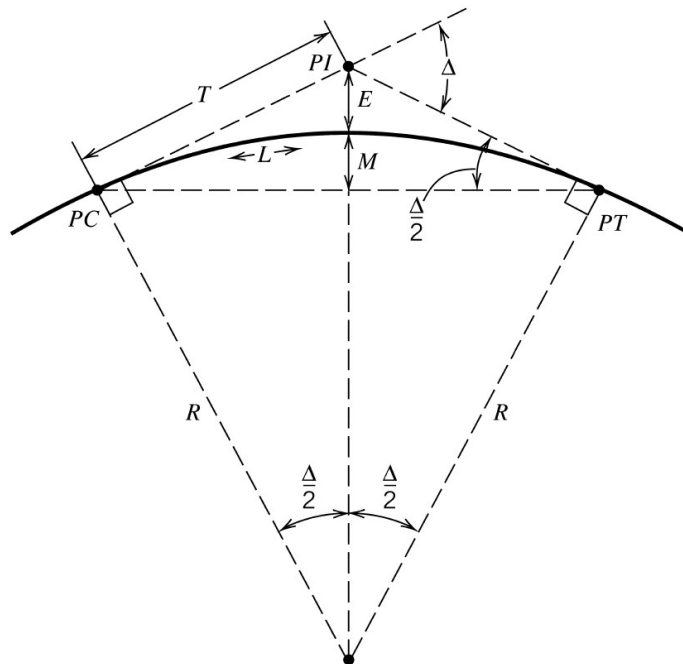


Figure 3-3: Typical Horizontal Alignment at Road Centerline (Mannering and Washburn 2013, 81)

Using the geometry of the alignment, the degree of curvature Δ may be calculated as either a function of the tangent T or the arc length L ;

$$\Delta = 2 \tan^{-1}(T / R)$$

or

$$\Delta = \left(\frac{180}{\pi} \right) \frac{L}{R}$$

Assuming that the curvature of the bridge matches that of the road centerline, the horizontal alignment of the bridge deck may be considered equivalent to that of the road (AASHTO 2012, 4-19). Therefore, the degree of curvature of the roadway is equivalent to that of the bridge deck.

Alternatively, the degree of curvature may be calculated by modeling the road centerline in CAD software. Using the northing and easting coordinates provided by the stake-out plans on the drawing sets, points were plotted in Autodesk AutoCAD software at the location the abutment and piers (Autodesk 2020). A horizontal alignment was created using approximate straight segments so that perpendicular lines could be made to represent the radius. The degree of curvature was then calculated using the AutoCAD dimensioning tools. The AutoCAD model for one of the bridges is presented in Figure 3-4.

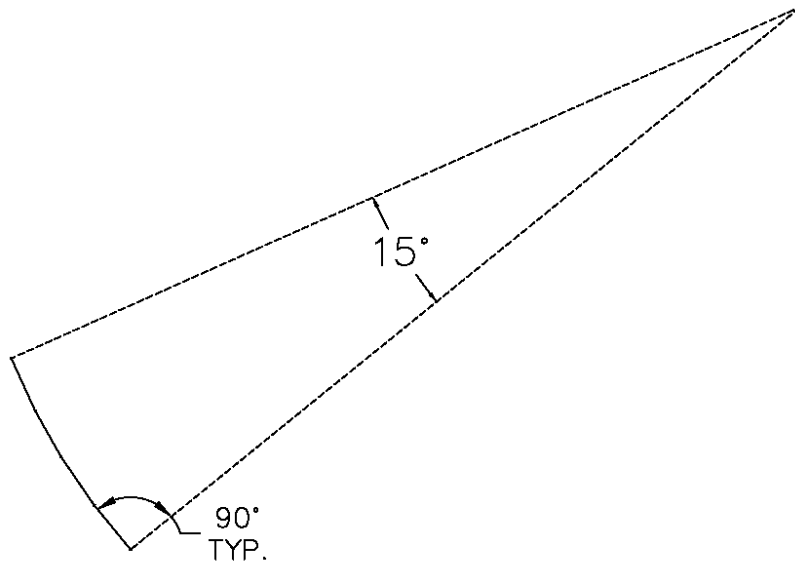


Figure 3-4: AutoCAD Horizontal Alignment

The degree of curvature for each bridge calculated using AutoCAD is presented in [Table 3-5](#).

Table 3-5: Degree of Curvature for Five Selected Bridges from Round One Selection Process

Road Carried	Deg. of Curvature (°)	Bridge Length	No. of Spans
PA State Road 15	5	162.26 m	4
PA State Road 0522 Sec. 5BS	6	128 ft	1
PA State Road 6219 NB	15	410 ft	4
PA State Road 15 NB	20	1087.33 ft	8
PA State Road 15 SB	23	846.21 ft	6

Of the five bridges, the bridge with a degree of curvature of 23° was selected for analysis using the developed finite element approach. By selecting a bridge with a large degree of curvature, the effects of curvature on the LLDFs would be amplified. Therefore, observations may be made on the effects of curvature on LLDFs for horizontally curved bridges with straight underlying girders.

3.3 Detail of the Selected Horizontally Curved Bridge

The bridge that was selected for analysis using the developed finite element approach is a six-span, 846 ft. long bridge with both six-girder and seven-girder sections and a 23° degree of curvature. Intermediate diaphragms were provided at mid-span for each of the six spans. Figure 3-5 presents an aerial view of the bridge from Google Maps (Google Maps n.d.). Figure 3-6 presents an elevation view of the bridge from the provided drawings (PennDOT 2005, 1). Figure 3-7 presents the bridge framing plan from the provided drawings. Figure 3-8 presents the transverse sections of the bridge.



Figure 3-5: Aerial View of Selected Horizontally Curved Bridge (Google Maps n.d.)

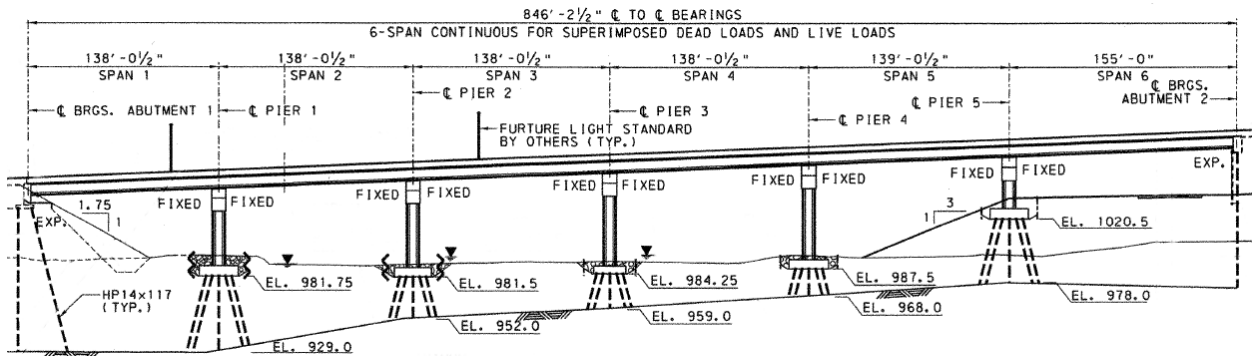
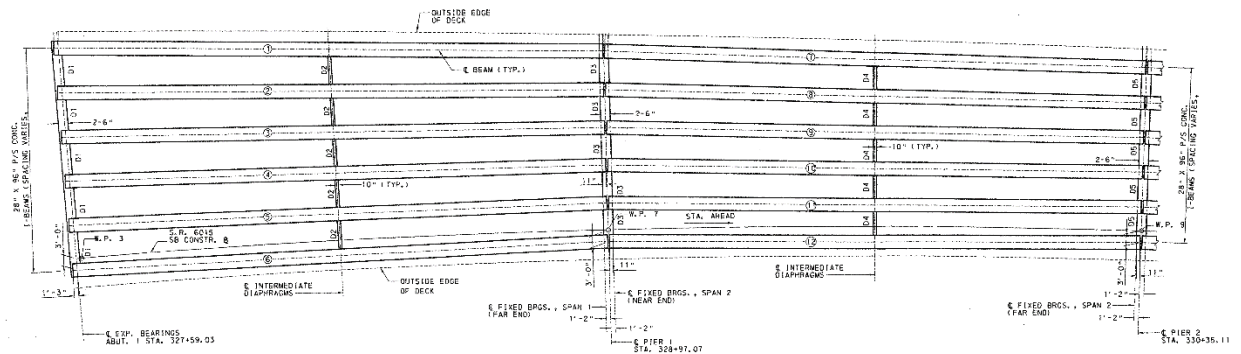
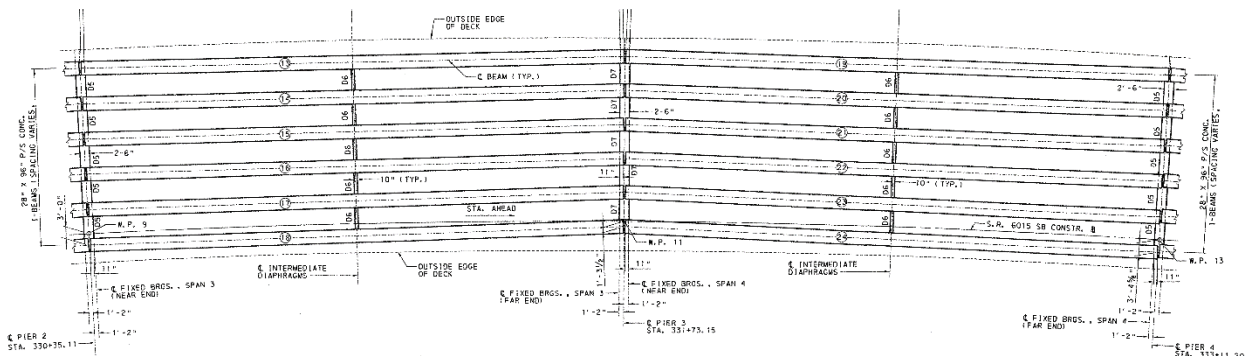


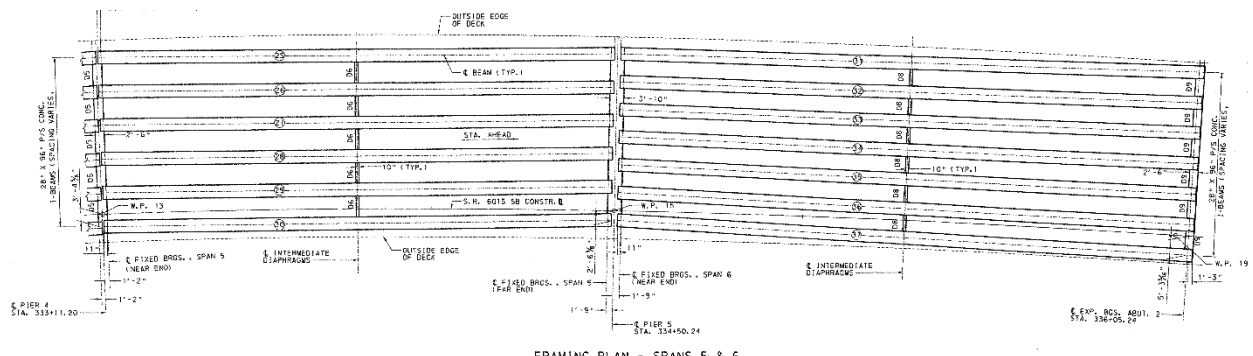
Figure 3-6: Elevation View of Selected Horizontally Curved Bridge (PennDOT 2005, 1)



FRAMING PLAN - SPANS 1 & 2



FRAMING PLAN - SPANS 3 & 4



FRAMING PLAN - SPANS 5 & 6

Figure 3-7: Framing Plan of Selected Horizontally Curved Bridge (PennDOT 2005, 31-33)

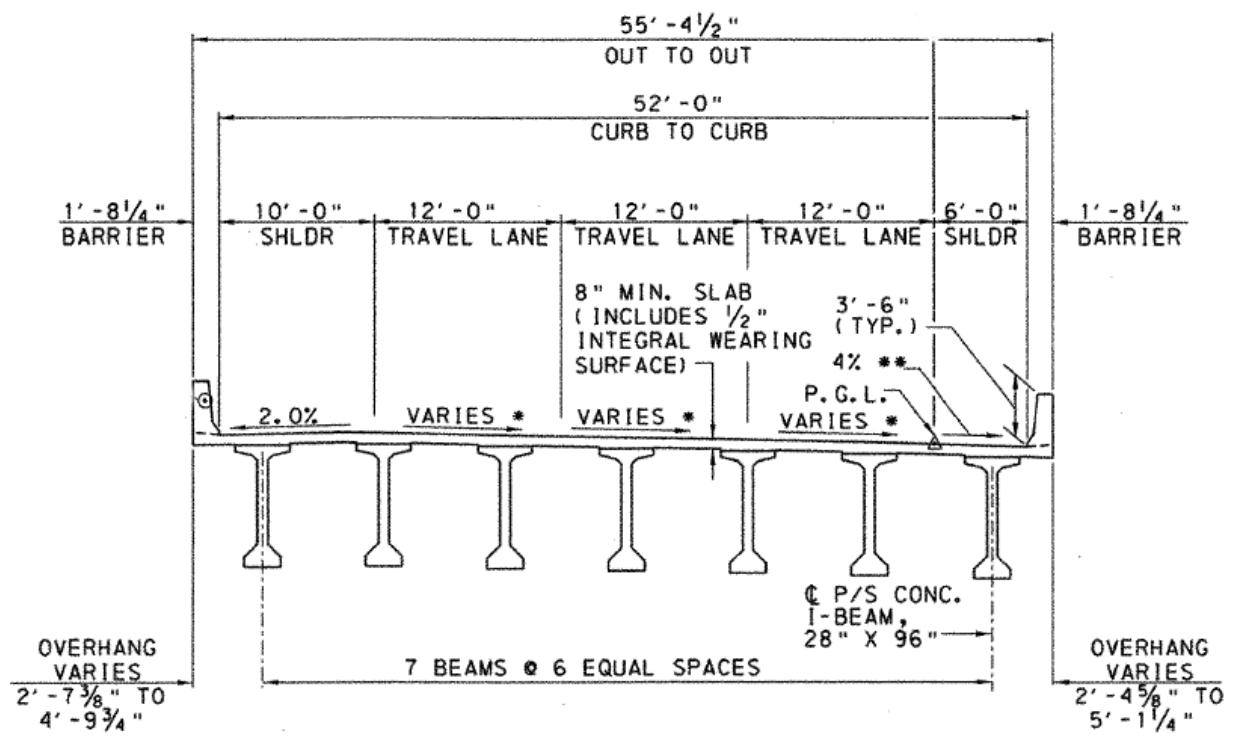
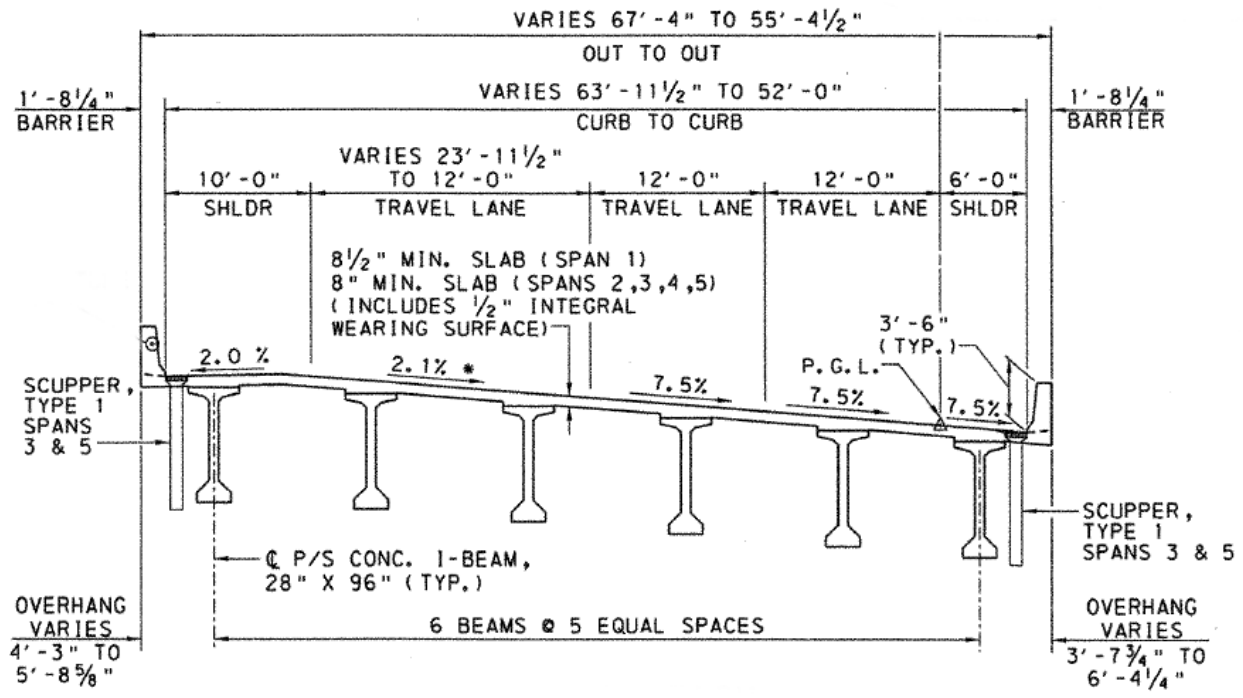


Figure 3-8: Transverse Sections of Selected Horizontally Curved Bridge (PennDOT 2005, 2)

The concrete strength of the bridge components is presented in Table 3-6.

Table 3-6: Concrete Strength for Bridge Deck and Girders of Selected Horizontally Curved Bridge

Concrete Deck, Cast-In-Place	$f'_c = 4000$ psi
Girders, Prestressed Precast Concrete	$f'_c = 8000$ psi

4 Simplification of Finite Element Models

Simplifications were developed for the generalized finite element approach that was applied to the selected bridge per suggestions from literature and the AASHTO specifications to limit the number of factors affecting load distribution, thus amplifying the effects of curvature on LLDFs. Additionally, geometric simplifications were made to the cross-sectional geometry and framing plans of the bridges to efficiently generate finite element models.

4.1 Simplification of Structural Components and Skew

Simplifications were developed using the provisions of AASHTO BDS and suggestions from literature to limit the factors affecting the LLDFs to amplify the effects curvature. The bridge models were simplified by removing secondary structural components, eliminating vertical curvatures, and eliminating skews.

Using the approximate equations shown in AASHTO BDS Article 4.6.2.2, the effects of secondary structural components on LLDFs were reviewed (AASHTO 2012, 4-33). Per AASHTO BDS Table 4.6.2.2.1-1 (Table 1-1), the selected horizontally curved bridge can be categorized using cross-section “k,” cast-in-place or precast concrete bulb sections. For two or more lanes loaded, the LLDF for interior girders is a function of the beam spacing, beam span, stiffness, and depth of the slab (AASHTO 2012, 4-33). The LLDF for exterior girders are a function of the interior girder LLDFs factors and a correction factor. This correction factor is calculated with the horizontal distance from the exterior beam centerline to the interior face of the parapet or other traffic barrier.

The substructure (abutments, piers, and foundation) was not modeled since the components (abutments, piers, and foundation) do not directly influence the load distribution factors per the AASHTO equations (Sotelino, et al. 2004, 24). The restraint mechanisms on the girders were included in the finite element models at the location of the piers.

The concrete parapets and traffic structures were removed from the finite element models in the interest of simplicity. Since the finite element approach is tailored for vehicular live loading to

calculate LLDFs, the concrete parapets and traffic structures are not necessary components since they only contribute to the bridge dead load (AASHTO 2012, 3-16).

Vertical curvature of the bridge and skew effects of the underlying girders were neglected in the finite element models. Per AASHTO BDS, girders on skewed supports have a reduced LLDF that can be calculated in accordance with AASHTO Table 4.6.2.2.2e-1, provided that the girder skews are within 10° of each other (AASHTO 2012, 4-40 - 4-41). Since only the effects of curvature were being investigated, removal of vertical curvature and skew effects that would contribute to the reduction of LLDFs was desirable to produce more conservative LLDFs.

4.2 Simplification of Horizontally Curved Bridge

Simplifications were made to the horizontally curved bridge per the AASHTO equations and suggestions from literature to amplify the effects of curvature by reducing factors which may impact the LLDFs.

The transverse width of the bridge deck was held constant at 55 ft. and 6 in., the narrowest width of the real bridge deck. This simplification was made so that the transverse positioning of the design lanes would remain constant along the entire bridge (AASHTO 2012, 3-17). A change in the position of the design lanes would impact the LLDFs since the HL-93 design loads would be positioned differently along the longitudinal span of the bridge.

The position of the underlying girders and number of girders was held constant. The real bridge has varying girder spacing at each pier and, at the last span, the number of underlying girders is increased to seven girders instead of six. A change in the transverse spacing of the girders will result in variation in the LLDFs per the lever rule and AASHTO equations (AASHTO 2012, 4-29). Since the girder spacing will vary with respect to the bridge deck because of the horizontal curvature of the deck, variation of transverse spacing at the piers was eliminated so that the effects of curvature on the LLDFs may be amplified. The transverse girder spacing was taken to be 9'-0", the average of the spacing at each pier of the real bridge.

The simplified transverse section of the horizontally curved bridge is presented in Figure 4-9. The framing plan of the horizontally curved bridge that was developed from these simplifications is presented in Figure 4-10. The simplified transverse section and simplified framing plan may

be compared to the actual transverse section (Figure 3-8) and actual framing plan (Figure 3-7) presented in Section 3.

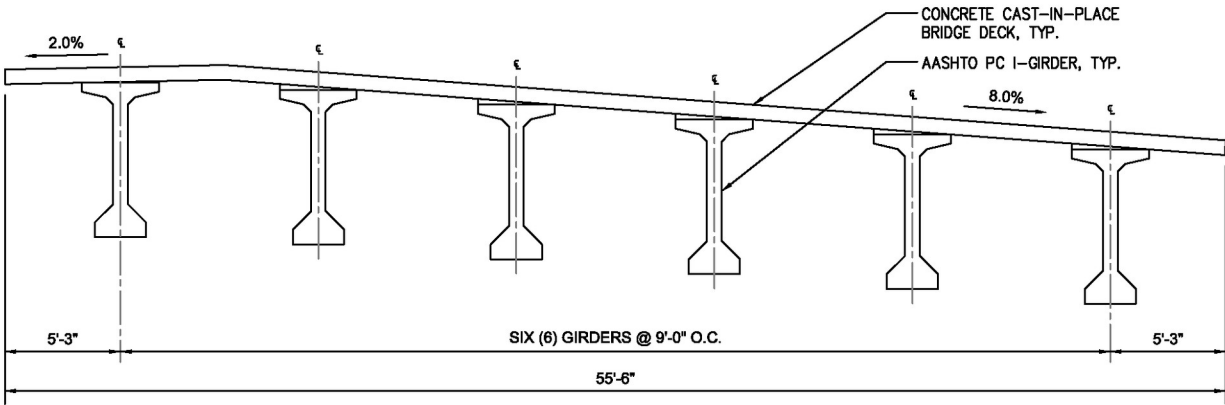


Figure 4-9: Simplified Transverse Section of Horizontally Curved Bridge

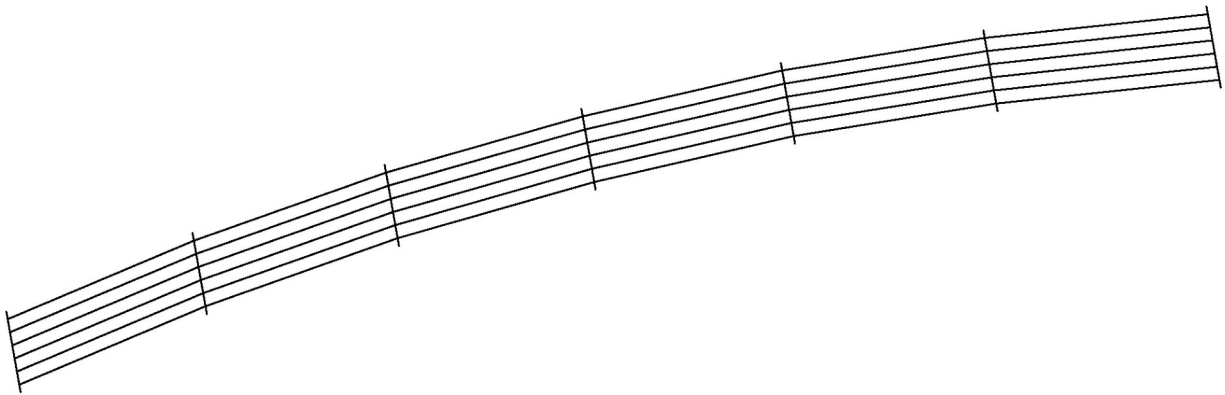


Figure 4-10: Simplified Framing Plan of Horizontally Curved Bridge

5 Finite Element Modeling of Bridge Geometry

Finite element models were created using the developed simplifications presented in Section 4. For the geometric modeling of the bridges, the structural software package SAP2000 by Computers and Structures, Inc. was used (CSI 2016). The developed approach for finite element modeling of the bridges is presented in the sub-sections below. The modeling approach was developed using provisions from AASHTO and the eccentric beam method, a popular method for modeling beam-slab bridges (Mensah 2006, 26).

5.1 Discretization of Elements

To create an accurate finite element model, the discretization, or mesh, size of the elements was calculated. AASHTO BDS categorizes discretization using an aspect ratio of the transverse dimension to the longitudinal dimension. AASHTO BDS Article 4.6.3 provides recommendations for the node placement and mesh aspect ratio for the bridge deck. Per AASHTO: the aspect ratio of finite elements and grid panels should not exceed 5.0, abrupt changes in size and shape of elements are to be avoided, and a minimum of five nodes per beam span is required (AASHTO 2012, 4-70).

Literature adds to the recommendations provided by AASHTO for the construction of more accurate finite element models. The fundamental study Chen & Aswad, 1996 established the following provisions for calculating mesh size (Chen and Aswad 1996, 114-115):

- Calculate transverse shell element length as half of the center-to-center spacing of the girders.
- Maintain an aspect ratio to 2.0 or less, reduced from the AASHTO requirement of 5.0 or less.
- Place nodes at the ends of a bridge, centerline of girders, and at evenly spaced intervals to maintain the calculated aspect ratio.

The discretization size of the elements for each bridge was calculated using the provisions from AASHTO and from literature along with additional considerations for model simplicity and shell

element connectivity. While literature recommended the transverse element length be half of the girder spacing, it is not required by the AAHSTO specifications (AASHTO 2012, 4-70). Therefore, to simplify the finite element models, the transverse element length for each bridge was taken as the spacing between the girders. For a 2:1 aspect ratio recommended by literature, the longitudinal element length was calculated as half of the transverse length and rounded to the nearest whole number in the interest of efficiently calculating node positions.

5.2 Calculation of Bridge Geometry

The geometry of each bridge was calculated as a series of nodes to which elements may be appended to create a finite element model. In SAP2000, 3D Cartesian coordinates for nodes are defined as x, y, and z. The x and y axes run horizontally, and the z axis runs vertically (CSI 2016, 15). The geometry of the bridge was calculated in the following order: location/orientation of bridge abutments and piers, plan geometry, and finally the elevation of bridge deck and underlying girders.

Using the northing and easting coordinates provided in the stake-out-plan of the construction drawings of each bridge, the angle of the abutment/piers and the distance between each abutment/pier was calculated. A coordinate transformation was then performed to translate the distances, calculated in reference to true north, to the Cartesian coordinate system.

The geometry of the bridge in plan was calculated using the located abutments/piers and the girder spacing presented in the simplified cross-sections shown in Section 4. In the transverse direction, nodes were calculated at the edges of the bridge deck and at the location of each girder centerline. The positions of these transverse nodes were then calculated at longitudinal intervals to maintain a 2:1 aspect ratio. For the straight girders, the position of the nodes was calculated using the equation of linear slope

$$y=mx+b$$

where x was the distance from the pier and y was the horizontal offset (Figure 5-11).

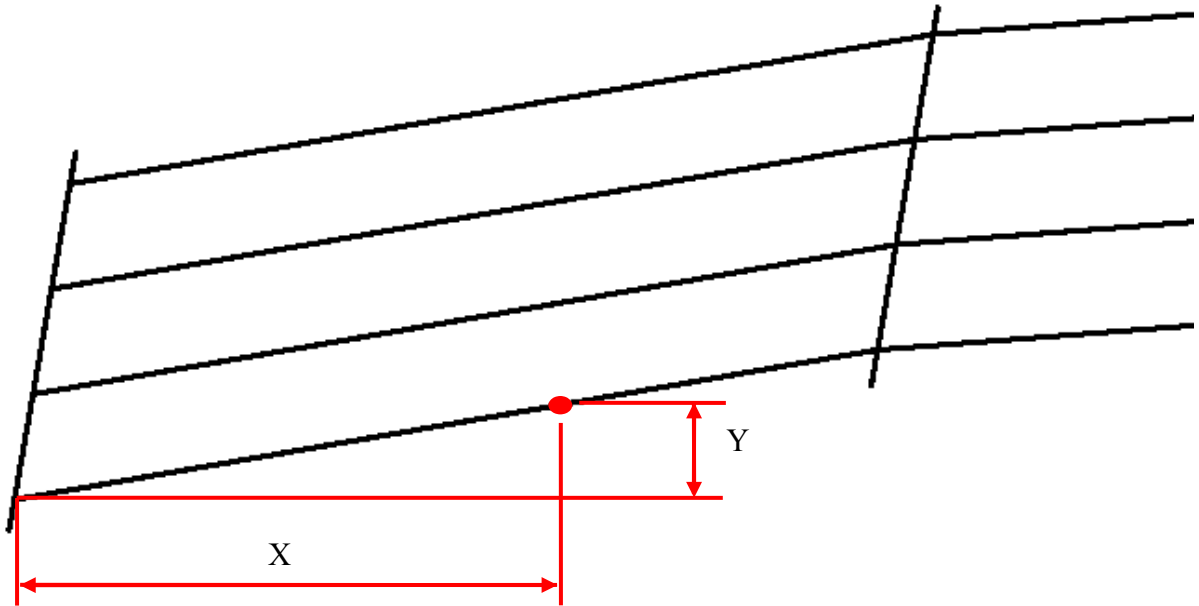


Figure 5-11: Girder Node Position

To calculate the nodes for the edges of the bridge deck, the horizontal curvature of the bridges was assumed to be a parabolic arc (Figure 5-12). For a parabolic arc, the position of the nodes is calculated using the equation

$$y = h \left(1 - \frac{x^2}{a^2} \right).$$

Using the distances between the abutments/piers as a and h , the curvature of the bridge deck can be approximated.

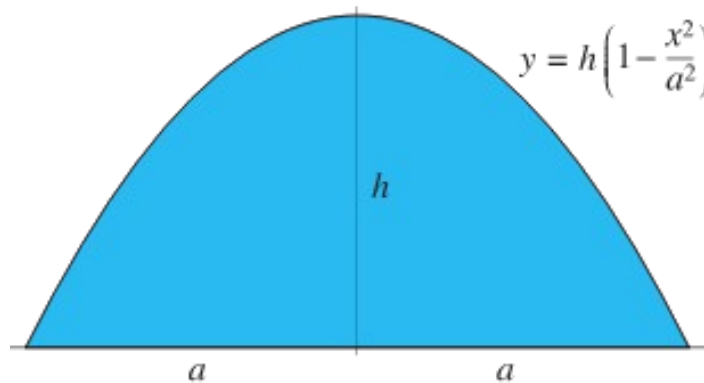


Figure 5-12: Parabolic Arc

Using the simplified cross-sections presented in Section 4, the elevation of each node was calculated. For each bridge deck node, the slope of the bridge deck was used to calculate the elevation as a function of the transverse distance. For the underlying girders, the nodes were placed at the centerline so that they may be connected to the bridge deck using rigid link elements (CSI 2016, 251-253). In plan, the underlying girder nodes were located using the same x and y coordinates as were calculated for the bridge deck. To calculate the elevation of the girder centerline relative to the bridge deck elevation, the distance from the top of the girder to the z-centroid was found and subtracted from the bridge deck elevation (AASHTO 2012, 4-70) (Chen and Aswad 1996, 115).

5.3 Definition of Element Types

In SAP2000, structural models are composed of objects with assigned properties and are then discretized into elements once analysis is conducted (CSI 2016, 8-9). In modern versions of the software, engineers may define parameters for automatic discretization. However, due to the complex geometry of the bridges modeled in this study, the elements were manually discretized with a one-to-one ratio of objects to elements (CSI 2016, 8).

AASHTO BDS Article 4.6.3, the provisions for refined analysis, does not dictate the types of elements that are to be used in finite element analysis. Instead, general provisions are detailed for assuming structural behavior in analysis and recommendations are made for the various types of refined analysis. Per suggestions from literature, shell elements, beam elements (referred to as frame elements in SAP2000), and links were used to model the structural features of the bridges using the eccentric beam method (Zaki 2016, 21-22) (Mensah 2006, 26). Using the eccentric beam method, the bridge deck and girders were modeled as four-node shell elements and two-node beam elements respectively with links connecting the nodes at the center of gravity (Mensah 2006, 26).

Shell elements were used to model the concrete bridge deck slab of the bridge. The shell elements used for modeling were rectangular four-node thin-shell elements with six degrees of freedom (DOF) at each node (Zaki 2016, 22) (Yousif and Hindi 2006, 7). Per AASHTO BDS Article 4.6.3.2.1, flexural and torsional deformation of the bridge deck must be considered in analysis while vertical shear deformation may be neglected (AASHTO 2012, 4-69). In SAP2000,

the thin-shell element neglects the vertical shear deformation and may be used when the thickness is less than one-tenth of the span (CSI 2016, 190-192). Additionally, the shell element was selected over the available plate element per the recommendations of CSI.

Prismatic frame elements, with no variation in sectional properties, were used to model the underlying concrete girders of the bridge (CSI 2016, 105-107). Per literature, the use of frame elements with nodes located at the center of gravity of the frame section and rigid link connection in SAP2000 is recommended for compatibility with moving load analysis and element force output (Yousif and Hindi 2006, 7-8). For the precast concrete bulb-tee sections used in each bridge, SAP2000 provides a menu to input specified dimensions. Figure 5-13 presents the SAP2000 section input menu for precast concrete bulb-tee members.

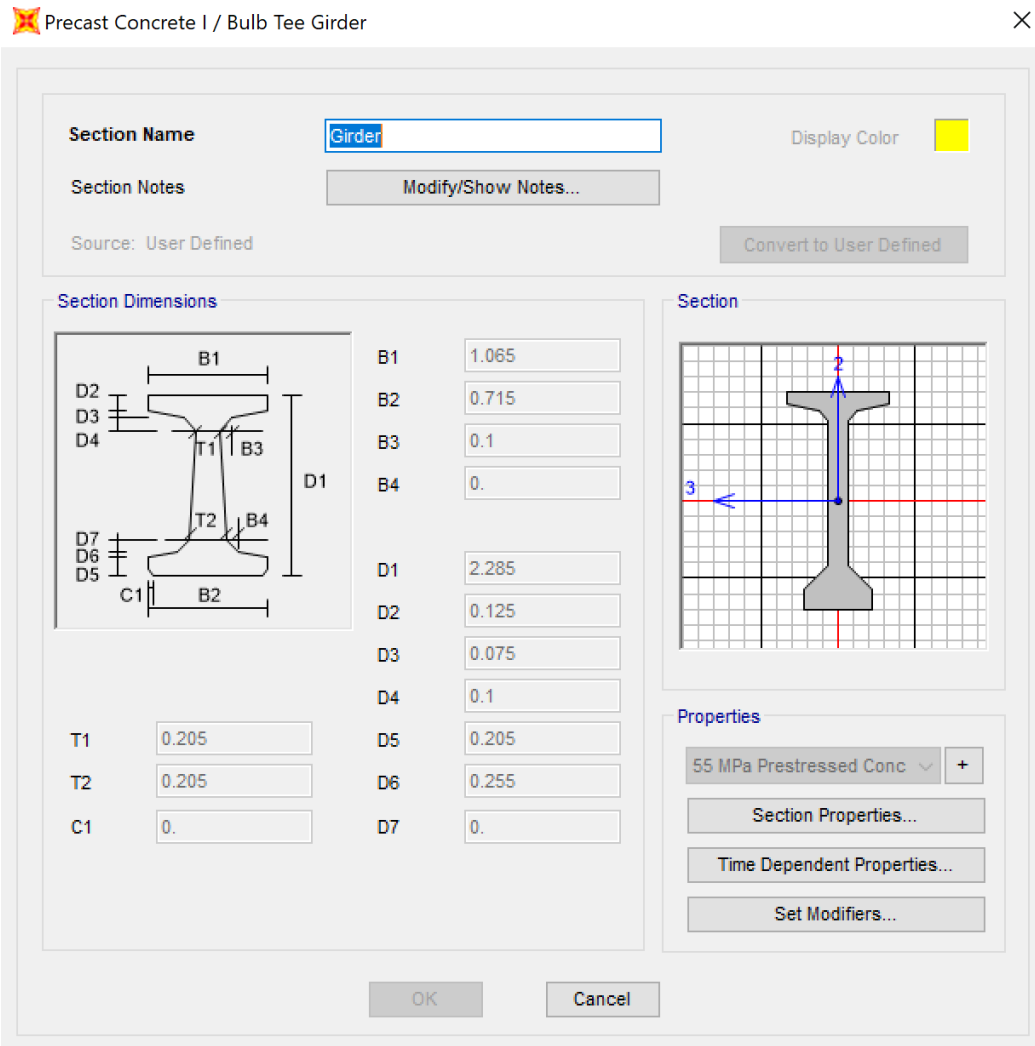


Figure 5-13: Precast Concrete Bulb-Tee Section Input Menu, SAP2000

Per AASHTO BDS Article C4.6.3.3.1, finite element models using shell and beam elements shall maintain the relative vertical distances between elements (AASHTO 2012, 4-70). Per the geometric node calculation procedure presented in Section 5.2, the position of the underlying girder nodes was calculated relative to the bridge deck. Since the shell elements and frame elements in SAP2000 were modeled separately and the spacing was kept between them, a link element was required for the finite element software to recognize the connection of the structural features and to simulate the known structural behavior (Yousif and Hindi 2006, 7). In SAP2000, a linear two-joint link element was used to connect the nodes of the bridge deck elements and the underlying girder elements located at the center of gravity (Yousif and Hindi 2006, 7). When

defining the link property, motion was restrained to properly model the composite behavior of the bridge deck and girders (Mensah 2006, 26).

To model the underlying mid-span diaphragms, the diaphragm constraint in SAP2000 was used. SAP2000 allows for the motion of nodes to be constrained to model rigid behavior and simulate nodes moving together as a rigid body (CSI 2016, 53). A specific diaphragm constraint may be applied to nodes to constrain rotation in any direction. For the mid-span diaphragms of the bridge, the girder nodes at each mid-span were constrained in the z-direction for rotation.

5.4 Finite Element Models

Using the developed approach, the horizontally curved bridge was modeled in SAP2000. To generate the finite element model, the interactive database editor within SAP2000 was utilized (CSI 2016). Using Microsoft Excel spreadsheets, the positions of each node and corresponding element assignments and properties were imported into SAP2000 and, from this data, the software generated a working finite element model (CSI 2004, 5-9). With the use of spreadsheets, finite element models created using this approach may be easily modified and re-generated as required.

The finite element model for the horizontally curved bridge created using the developed modeling approach is presented in Figure 5-14.

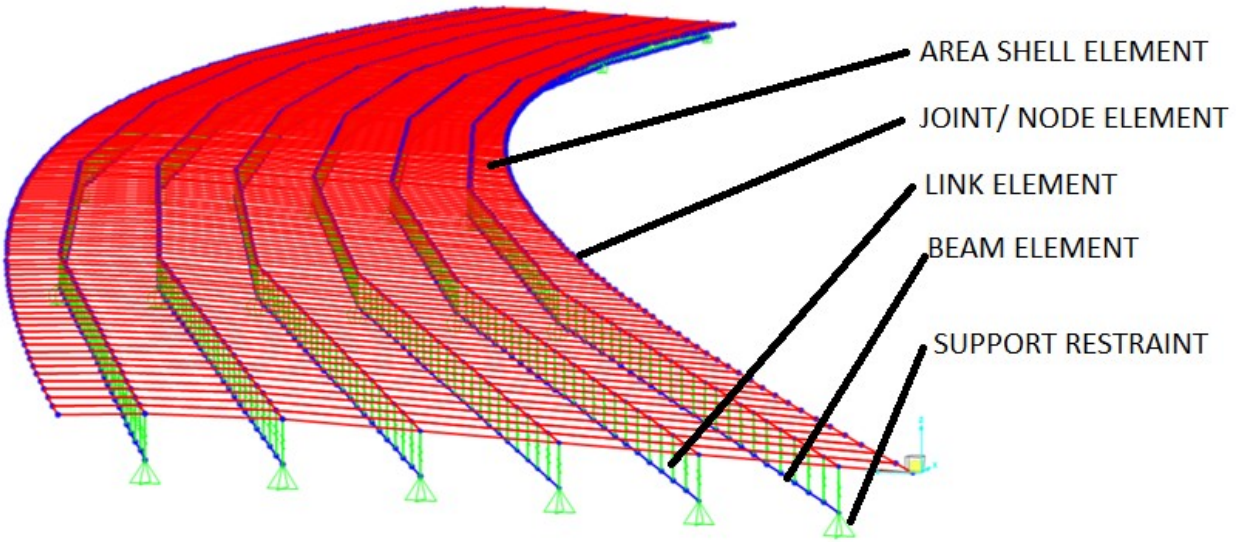


Figure 5-14: Finite Element Model of Horizontally Curved Bridge

To analyze the effect of curvature on LLDFs, the developed finite element modeling methods were used to create a straight bridge model using the same span length, material properties, sectional properties, and cross-sectional geometry as the horizontally curved bridge. The finite element model for the straight bridge is presented in Figure 5-15.

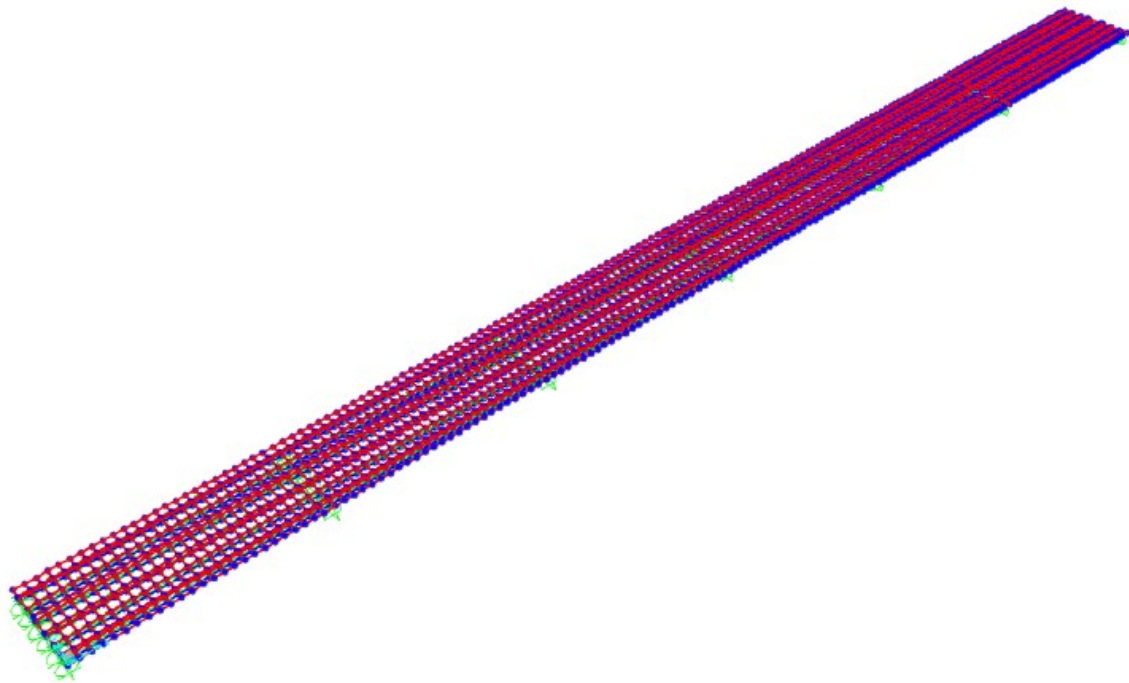


Figure 5-15: Finite Element Model of Straight Bridge

5.5 Verification of Finite Element Modeling Methods

The accuracy of the developed approach for creating finite element models was tested using a small-scale test bridge model and accompanying hand calculations. The test bridge that was used for verification of finite element methods is presented in Figure 5-16.

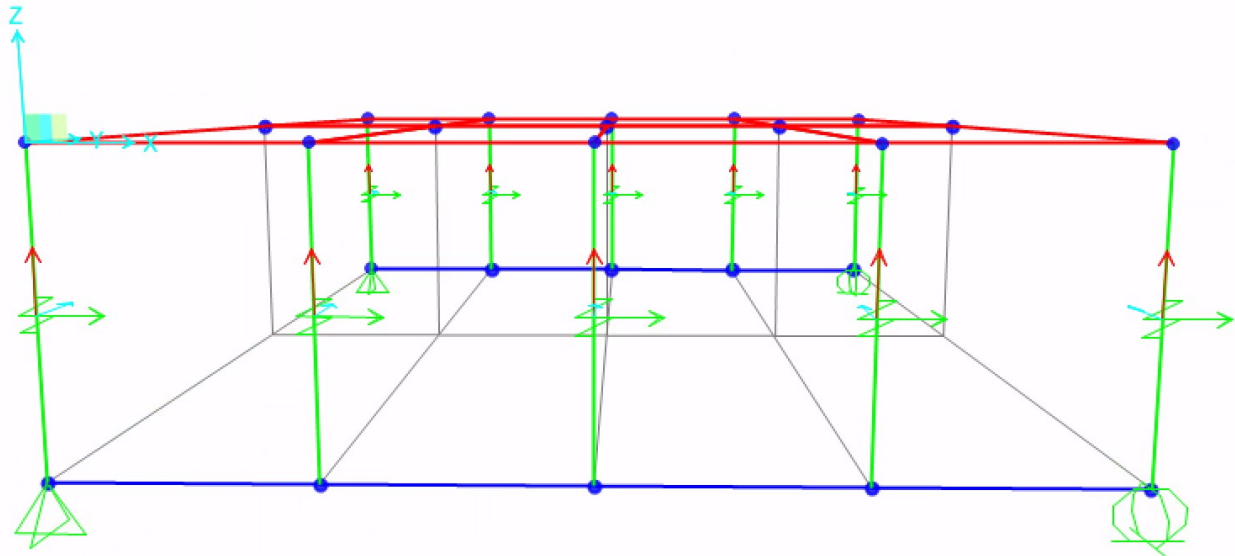


Figure 5-16: Test Bridge

As presented in Figure 5-16, the test bridge is simply supported with two girders at the extreme edges of the bridge. The longitudinal span of the bridge is 4m and the transverse width is 5m. An aspect ratio of 2.5:1 was used as the mesh size.

A simple structural analysis was conducted in SAP2000 and by hand using a 0.5 kN/m^2 area load applied on the bridge deck to verify the load transfer from the bridge deck to the underlying girders using the link elements simulating composite behavior. The moment diagrams generated from both methods were then compared. If the link elements were configured properly, the load from the bridge deck would be transferred to the bridge girders without inducing any additional forces.

For the hand calculation, the area load was converted to concentrated loads at each node with a link element using the tributary area. The resulting loads P_{EXT} and $P_{f\Box}$, for the exterior links and interior links respectively, were then placed onto the underlying girder and the moment diagram

was drawn. The calculations performed to calculate the loads transferred to the girders are presented below.

$$P_{EXT} = TA * 0.5 \text{ kN/m}^2 = (2.5 \text{ m} * 0.5 \text{ m}) * 0.5 \text{ kN/m}^2 = 0.625 \text{ kN}$$

$$P_{\int \square} = TA * 0.5 \text{ kN/m}^2 = (2.5 \text{ m} * 1 \text{ m}) * 0.5 \text{ kN/m}^2 = 1.25 \text{ kN}$$

The moment diagram calculated by hand and by SAP2000 is presented in Figure 5-17.

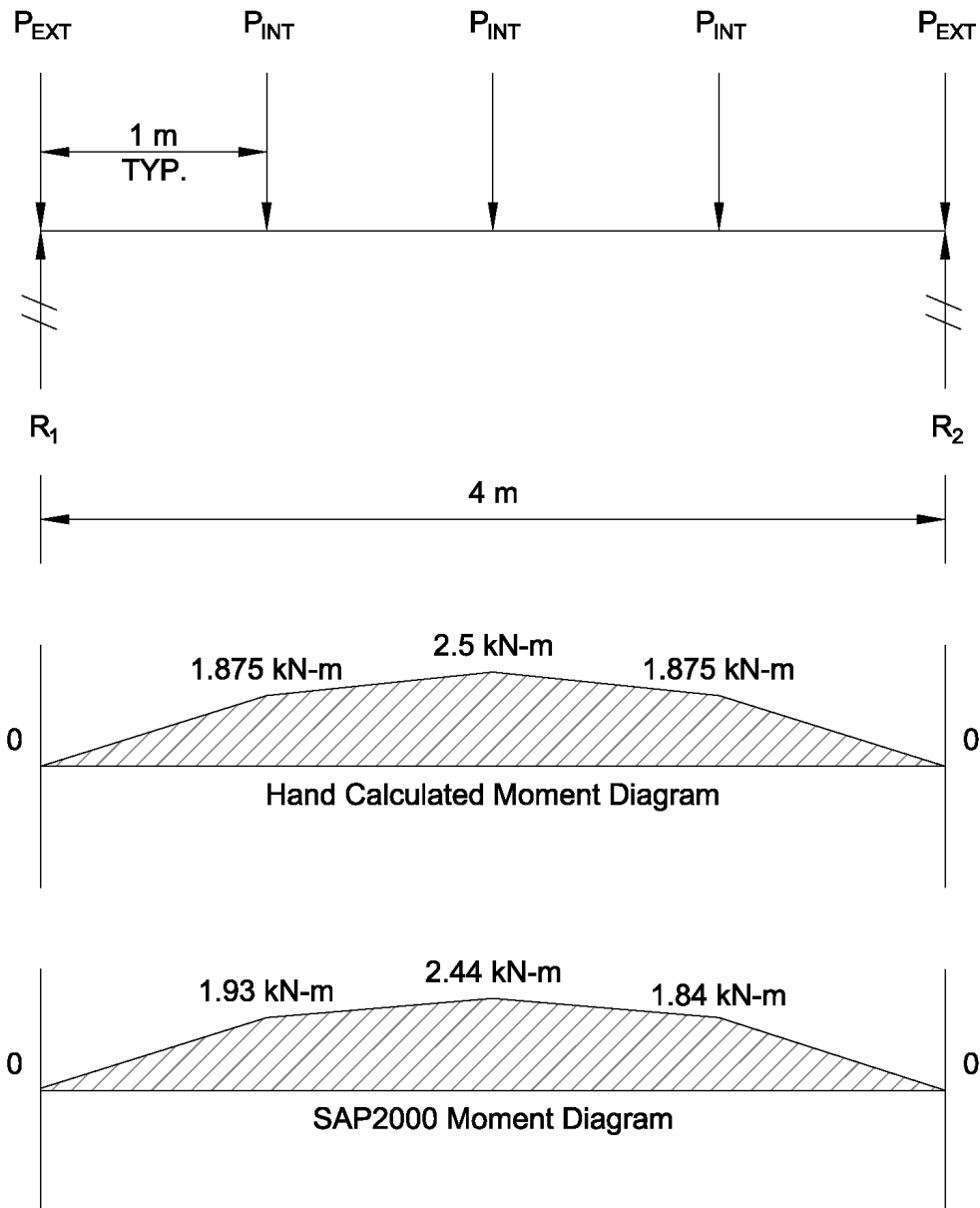


Figure 5-17: Test Bridge Moment Diagrams

The moment diagrams generated by SAP2000 matched the results of the hand calculated moment diagram with a difference of only 3%. This difference may be attributed to added girder self-weight from the default frame section used in SAP2000 as well as force effects in the deck slab that would result in a slightly uneven distribution of load transferred through the link elements. However, this variation did not cause a significant difference in the moment diagrams (Nowak 2018).

Along with verifying the modeling methods, this test also reveals the importance of the mesh size. As seen in the test, the load is transferred down to the underlying girders at the location of each link. In actuality, the load is transferred continuously in the longitudinal direction from the bridge deck to the underlying girders. Per structural analysis, this would result in the moment diagram for the underlying girder being a second order curve since the load that would be transferred from the deck would act as a line load. Instead, the moment diagram developed by the software is a linear approximation of the second order curve with the concentrated loads transferred through the link elements. Therefore, minimizing the aspect ratio of the finite element model results in a more accurate approximation of the force effects by increasing the number of links to the underlying girders.

6 Live Loading and Calculation of LLDFs

Vehicle live load was applied per the provisions of AASHTO BDS to the finite element models created using the approach presented in Section 5. To compare the difference in moving load capability between SAP2000 and CSiBridge, live loading was done with the two software packages using influence-based moving load analysis (CSI 2022) (CSI 2016). The methods used to apply live load to the finite element models were verified using an example bridge designed by the U.S. Federal Highway Administration (FHWA) with provided LLDFs calculated using the AASHTO BDS provisions (FHWA 2015, 2-1 - 2-11).

6.1 Load Cases for Horizontally Curved Bridge

The AASHTO BDS provisions were used to determine the load cases that would be applied to the bridge models. Per AASHTO BDS Article 3.6.1.1.2, all possible combinations of loaded design lanes must be applied to the bridge models so that the largest possible forces will be considered in design (AASHTO 2012, 3-24). Additionally, each combination of loaded design lanes must be multiplied by the multiple presence factors presented in AASHTO BDS Table 6.1.1.2-1.

The maximum number of design lanes for the horizontally curved bridge was calculated using the AASHTO provisions. Per AASHTO BDS Article 3.6.1.1, the number of 12 ft. wide design lanes for a bridge deck is the clear roadway width in feet divided by 12 (AASHTO 2012, 3-17). Using the roadway width of the simplified transverse section presented in Figure 4-9, the maximum number of design lanes per the AASHTO provisions for the horizontally curved bridge is four 12 ft. lanes.

Per AASHTO, all possible combinations of loaded design lanes must be considered (AASHTO 2012, 3-18). For the horizontally curved bridge with four design lanes, 15 load combinations presented themselves. The list of load combinations and multiple presence factors for the horizontally curved bridge is presented in Table 6-7. An illustration of the location of the design lanes on the bridge is presented in Figure 6-24 in Section 6.3.

Table 6-7: Live Load Combinations for Horizontally Curved Bridge

No. of Possible Combinations	Lanes Loaded	Multiple Presence Factor “<i>m</i>” (AASHTO BDS Table 6.1.1.2-1)
4	1 of 4 Lanes Loaded	1.20
6	2 of 4 Lanes Loaded	1.0
4	3 of 4 Lanes Loaded	0.85
1	All Lanes Loaded	0.65

6.2 Live Loading Using SAP2000

The finite element models for the horizontally curved bridge and straight bridge were loaded and analyzed using the vehicle and moving load tools in SAP2000. To simulate vehicle loading, the program applies a user-defined vehicle over a path that is defined from specified beam elements (CSI 2016, 479-480). Vehicles can be input as a series of concentrated or uniform loads acting in the direction of gravity. In SAP2000, vehicles can only be defined in the longitudinal direction. Functionality to define transverse features of vehicles, such as axle width and transverse lane load, is limited to CSiBridge (CSI 2016, 479-480).

To apply the AASHTO HL-93 load and design truck to the bridge models, user-defined paths were placed on the bridge deck to represent the design lanes. In SAP2000, paths are defined using a series of beam elements. The software then applies the vehicle load over the path with user-defined moving load cases (CSI 2016, 509-510). Since the full HL-93 design load could not be consolidated into a single vehicle, additional paths were required to simulate the full design truck. For each design lane, three paths were defined; one path for the center of the lane and two paths spaced at 6 ft. to simulate the full design truck.

The HL-93 vehicle load was inputted into the finite element models. To generate the maximum positive and negative moments during structural analysis, the HL-93K and HL-93S design trucks were used (Zaki 2016, 22-24). The HL-93K load consists of the HL-93 design truck presented in Figure 1-1 and, when applied to the bridge models, will generate the maximum positive moment. The HL-93S load consists of two HL-93 design trucks spaced at a minimum of 50 ft. to generate the maximum negative moment. The HL-93K and HL-93S loads defined in SAP2000 are presented in Figure 6-18.

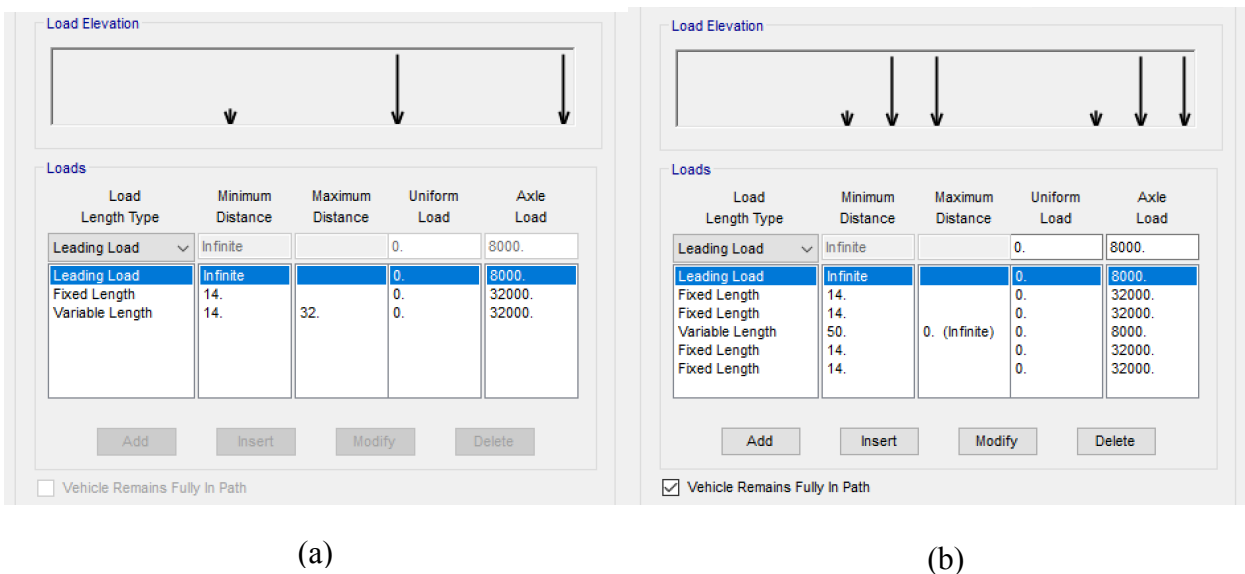


Figure 6-18: (a) HL-93K & (b) HL-93S Vehicle Loads in SAP2000 (In Pounds)

To calculate the geometric position of the nodes and beam elements for the paths, the approach presented in Section 5 was used. To ensure transfer of live load from the bridge deck to the underlying girders, the deck shell was re-meshed so that the nodes linking the deck to the girders and the nodes of the vehicle paths were connected (Barr, Eberhard and Stanton 2001, 300). Additionally, the beam elements of the vehicle path that vehicles would travel over were defined with no sectional properties so that SAP2000 would not assume that the beam elements were structural components. Figure 6-19 presents the finite element model of the horizontally curved bridge with the re-meshed bridge deck. Figure 6-20 presents the finite element model of the straight bridge with the re-meshed bridge deck.

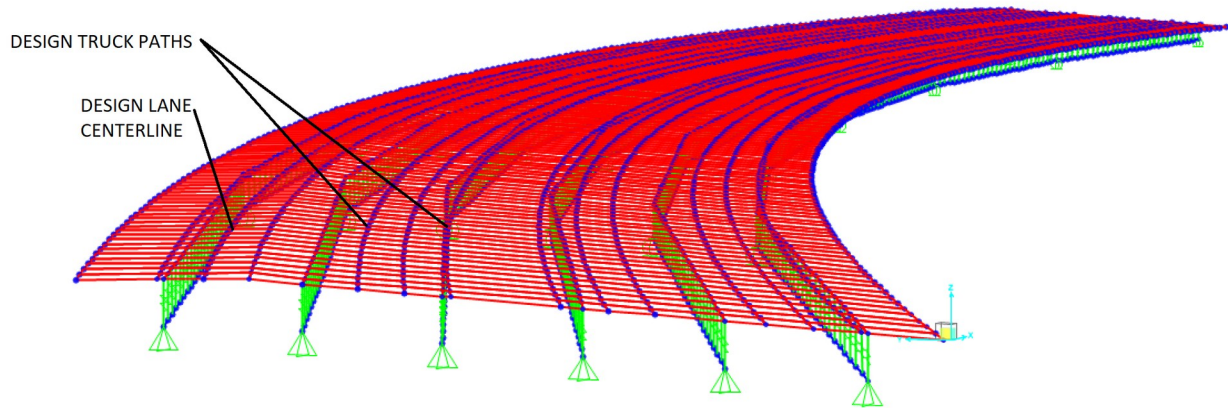


Figure 6-19: SAP2000 Finite Element Model of Horizontally Curved Bridge with Lanes

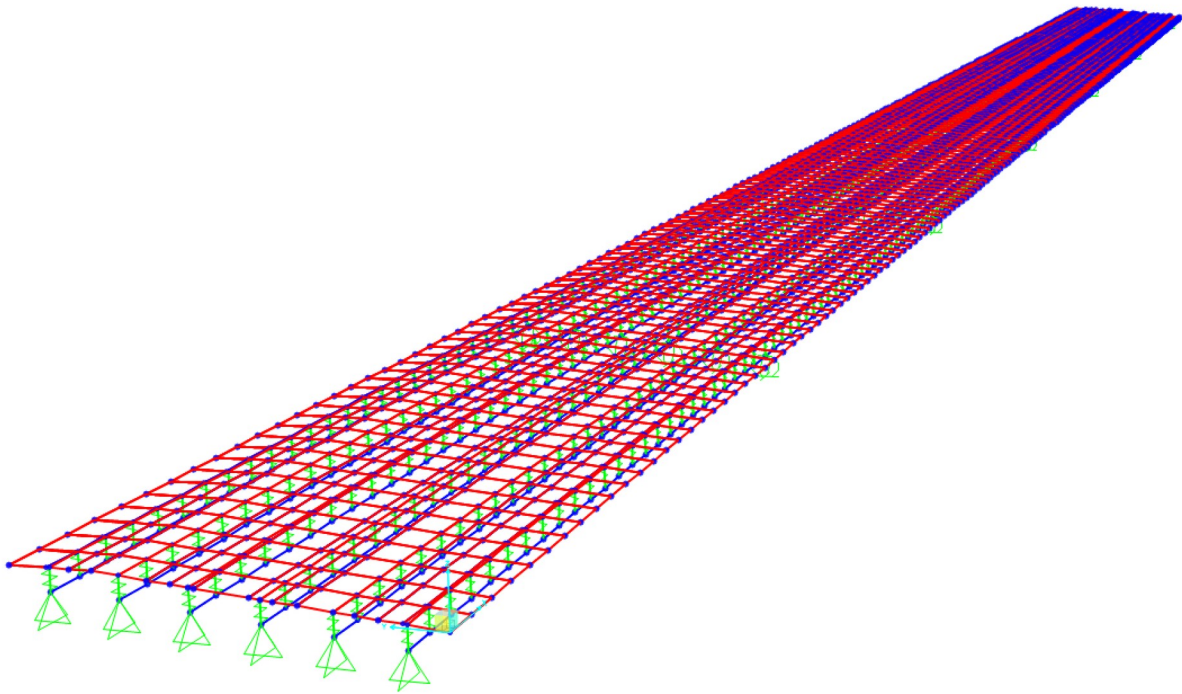


Figure 6-20: SAP2000 Finite Element Model of Straight Bridge with Lanes

Once the paths for each design lane were defined, the moving load cases for each of the 15 load combinations (Table 6-7) were defined. SAP2000 allows for moving load analysis to be conducted as either a multi-step linear static analysis or an influence-based analysis. When using CSiBridge, it is recommended that influence-based analysis be used due to the consideration of transverse effects and vehicle placement at each lane by the software (CSI 2016, 481). Since SAP2000 does not provide the functionality to move the vehicles transversely, this

recommendation by CSI is not applicable. However, the influence-based analysis was preferable to the multi-step analysis. Multi-step analysis in SAP2000 does not consider variable axle spacing which is used in the HL-93K and HL-93S loads (CSI 2016, 481-482). Additionally, any uniform loads are not considered in the analysis which would exclude the lane load required per AAHSTO. Therefore, influence-based analysis was used for the live loading in SAP2000.

For influence-based analysis in SAP2000, the “Moving Load” load case was used to apply the HL-93 vehicle load over the design lanes (CSI 2016). For each of the load combinations, both the HL-93K and HL-93S trucks were loaded onto the appropriate number of paths and the multiple presence factor was applied as required. The input menu for the moving load case of all lanes loaded is presented in Figure 6-21.

Load Case Name
MOVE15 [Set Def Name] [Modify/Show...]

Notes

Load Case Type
Moving Load [Design...]

Stiffness to Use
 Zero Initial Conditions - Unstressed State
 Stiffness at End of Nonlinear Case
 Important Note: Loads from the Nonlinear Case are NOT included in the current case

Directional Factors
1. [] [] []

MultiPath Scale Factors
 Number of Paths Loaded: 1 []
 Reduction Scale Factor: 1. [] 1. [] 0.65 [] [Modify]

Loads Applied

Assign Number	Vehicle Class	Scale Factor	Min Loaded Paths	Max Loaded Paths	Paths Loaded
1	HL-93	1.	8	8	Some

[Add] [Modify] [Delete]

Paths Loaded for Assignment 1

List of Path Definitions	Selected Path Definitions
Lane1_Center	L1_BotWheel
Lane2_Center	L1_TopWheel
Lane3_Center	L2_BotWheel
Lane4_Center	L2_TopWheel

Mass Source
MSSSRC1

[OK] [Cancel]

Figure 6-21: Moving Load Case Definition - SAP2000

To apply the design lane load of 0.640 k/ft to each design lane, a separate live load case was created for each lane using a uniform distributed load at the center of the lane. To simulate the full HL-93 loading in SAP2000, the moving load cases and the design lane load cases were combined into 15 different load combinations. With these load combinations, structural analysis was conducted on the finite element models. The deformed shape of the horizontally curved bridge and straight bridge for all lanes loaded is presented in Figure 6-22.

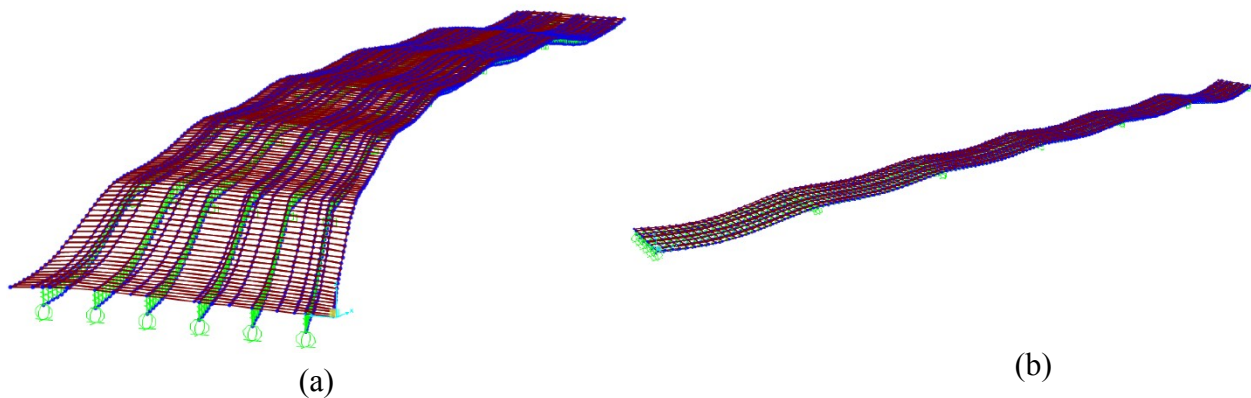


Figure 6-22: Live Load Deformation for (a) Horizontally Curved Bridge & (b) Straight Bridge for All Design Lanes Loaded

6.3 Live Loading Using CSiBridge

The finite element models for the horizontally curved bridge and straight bridge were loaded and analyzed using the vehicle and moving load tools in CSiBridge (CSI 2022). For the definition of vehicles, CSiBridge provides a list of standard design vehicles from different countries and codes which can be imported into model files and used for moving load analysis (CSI 2016, 500-507). The AASHTO HL-93K and HL-93S vehicles and for generating maximum positive moment and maximum negative moment are included in CSiBridge. The HL-93K and HL-93 loads provided by CSiBridge are presented in Figure 6-23.

Vehicle Name: HL-93K Design Type: Vehicle Live Units: lb, ft, F

Source: AASHTO.xml Convert to User Defined Notes: Notes...

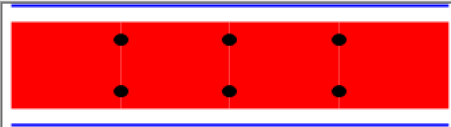
Length Effects
 Axle: None Modify/Show...
 Uniform: None Modify/Show...

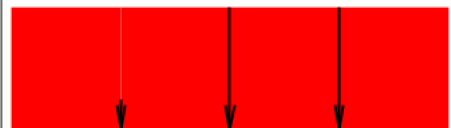
Vehicle Location in Lane
 Vehicle Applies To Straddle (Adjacent) Lanes Only
 Straddle Reduction Factor:
 Vehicle Remains Fully In Lane (In Lane Longitudinal Direction)

Usage
 Lane Negative Moments at Supports
 Interior Vertical Support Forces
 All other Responses

Min Dist Allowed From Axle Load
 Lane Exterior Edge: 1.
 Lane Interior Edge: 2.

Center of Gravity
 Height - Axle Loads: 0.
 Height - Uniform Loads: 0.

Load Plan: 

Load Elevation: 

Modify/Show Loads
 Vertical Loading... Horizontal Loading...

OK Cancel

Vehicle Name: HL-93S Design Type: Vehicle Live Units: lb, ft, F

Source: AASHTO.xml Convert to User Defined Notes: Notes...

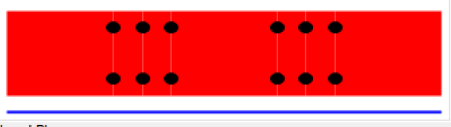
Length Effects
 Axle: None Modify/Show...
 Uniform: None Modify/Show...

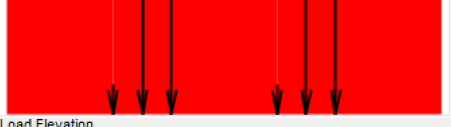
Vehicle Location in Lane
 Vehicle Applies To Straddle (Adjacent) Lanes Only
 Straddle Reduction Factor:
 Vehicle Remains Fully In Lane (In Lane Longitudinal Direction)

Usage
 Lane Negative Moments at Supports
 Interior Vertical Support Forces
 All other Responses

Min Dist Allowed From Axle Load
 Lane Exterior Edge: 1.
 Lane Interior Edge: 2.

Center of Gravity
 Height - Axle Loads: 0.
 Height - Uniform Loads: 0.

Load Plan: 

Load Elevation: 

Modify/Show Loads
 Vertical Loading... Horizontal Loading...

OK Cancel

Figure 6-23: (Top) HL-93K & (Bot.) HL-93S Vehicle Loads in CSiBridge

To apply the HL-93 load to the bridge models, lanes were defined to represent the four design lanes. In CSiBridge, the centerline of a lane can be defined using either bridge layout lines or beam elements (CSI 2016, 482). To keep parity with the loading methods used with SAP2000, lanes were defined using beam elements. To calculate the geometric position of the nodes and beam elements for the lanes, the approach presented in Section 5 was used. To ensure transfer of live load from the bridge deck to the underlying girders, the deck shell was re-meshed so that the nodes linking the deck to the girders and the nodes of the lane centerline were connected (Barr, Eberhard and Stanton 2001, 300). Additionally, the beam elements of the lane centerline were defined with no sectional properties so that CSiBridge would not assume that the beam elements were structural components. Figure 6-24 presents the finite element model of the horizontally curved bridge with the re-meshed bridge deck. Figure 6-25 presents the finite element model of the straight bridge with the re-meshed bridge deck.

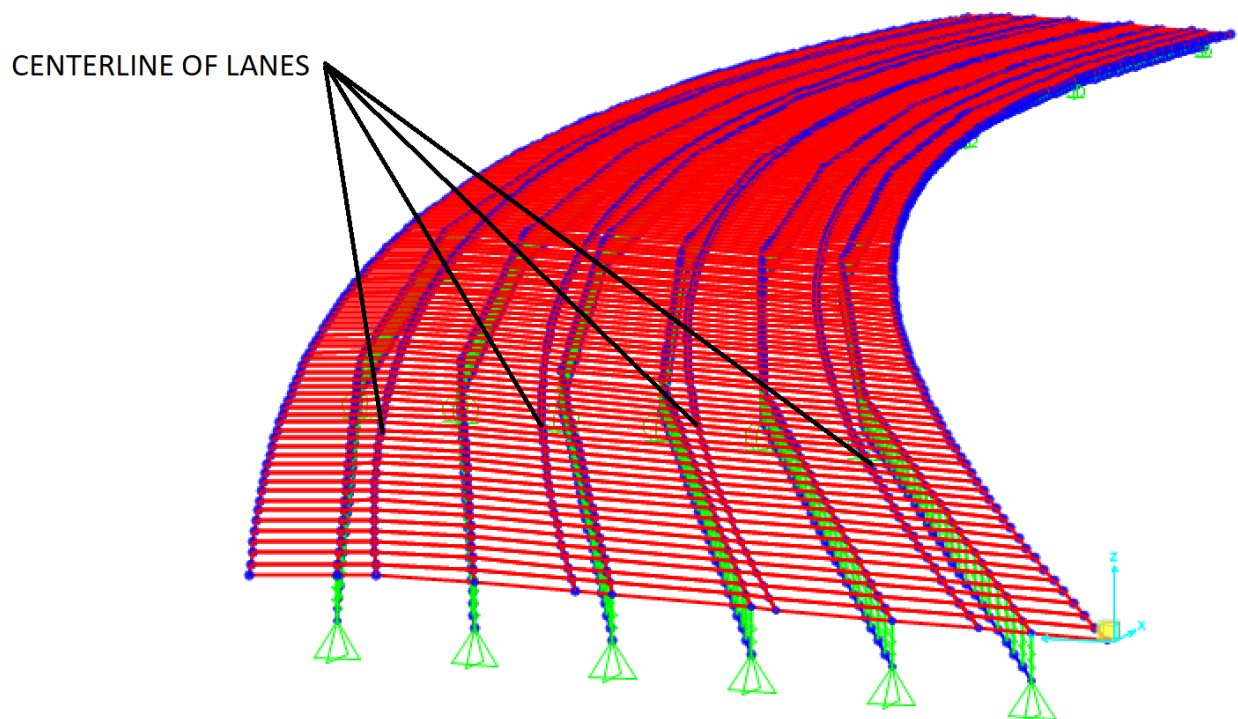


Figure 6-24: CSiBridge Finite Element Model of Horizontally Curved Bridge with Lanes

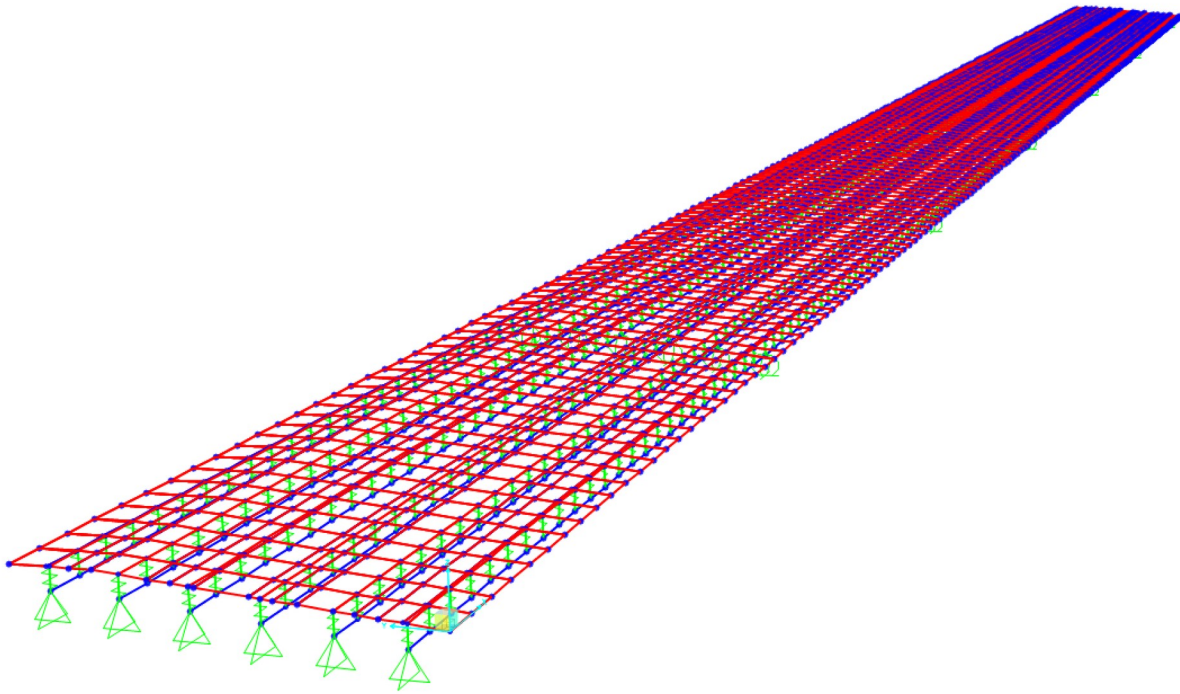


Figure 6-25: CSiBridge Finite Element Model of Straight Bridge with Lanes

Once the design lanes were defined, the moving load cases for each of the 15 load combinations (Table 6-7) were defined. CSiBridge allows for moving load analysis to be conducted as either a multi-step linear static analysis or an influence-based analysis. It is recommended that influence-based analysis be used due to the consideration of transverse effects and vehicle placement at each lane by the software (CSI 2016, 481). Additionally, multi-step analysis does not consider either variable axle spacing or uniform loads which are used in the HL-93K and HL-93S loads (CSI 2016). Therefore, influence-based analysis was used.

For influence-based analysis in CSiBridge, the “Moving Load” load case was used to apply the HL-93 vehicle load over the design lanes (CSI 2016). For each of the load combinations, both the HL-93K and HL-93S trucks were loaded onto the appropriate number of paths and the multiple presence factor was applied as required. The input menu for the moving load case of all lanes loaded is presented in Figure 6-26. With all load cases defined, structural analysis was conducted on the finite element models.

Load Case Name: MOVE15

Load Case Type: Moving Load

Stiffness to Use: Zero Initial Conditions - Unstressed State

Directional Factors: Vertical (1.0), Braking/Acceleration, Centrifugal

Assign Number	Vehicle Class	Scale Factor	Min Loaded Lanes	Max Loaded Lanes	Lanes Loaded
1	HL-93	1.	4	4	All

Number of Lanes Loaded	Reduction Scale Factor
1	1
2	1.2
3	0.85
4	0.65

Lanes Loaded for Assignment 1: Selected Lane Definitions: Lane1_Center, Lane2_Center, Lane3_Center, Lane4_Center

Mass Source: MSSSRC1

Figure 6-26: Moving Load Case Definition - CSiBridge

6.4 Calculation of LLDFs

The raw structural analysis data produced by SAP2000 and CSiBridge for the beam elements representing the underlying girders was exported to Microsoft Excel and sorted to calculate the LLDFs for each bridge model. In Excel, the raw structural analysis data was sorted so that the maximum positive moment and maximum negative moment may be viewed for each beam element for each load combination. Additionally, the underlying girder that corresponded with each beam element was marked and was placed into separate spreadsheets for each underlying girder.

LLDFs were calculated for each girder for each of the 15 load combinations. To calculate the LLDFs, the maximum positive and negative bending moments of each individual girder was compared to the maximum positive and negative bending moments generated by the full effect of the HL-93 loading (Zaki 2016, 27). LLDFs were calculated using the equation

$$\text{LLDF} = \frac{M_{\text{max, girder}}}{M_{\text{max}}}$$

where $M_{\text{max, girder}}$ is the maximum positive or negative bending moment of each individual girder and M_{max} is the maximum positive or negative bending moment generated by the full effect of the HL-93 loading. To simulate the full effect of the HL-93 load, the HL-93K and HL-93S loads were applied to a single girder of the bridge models in both SAP2000 and CSiBridge (Barr, Eberhard and Stanton 2001, 301-302) (Zaki 2016, 27). Using Excel, calculations were then performed to calculate the LLDFs for positive moment and for negative moment with the above equation. From the calculated LLDFs for each load combination, the controlling LLDFs were found and tabulated. Controlling LLDFs were classified as the maximum LLDF for interior and exterior girders for one lane loaded, two lanes loaded, three lanes loaded, and all four lanes loaded (Zaki 2016, 35).

6.5 Verification of Definition of Live Loads

The accuracy of the methods used for applying the AASHTO HL-93 load to the bridge models was verified using an example bridge designed by the US Federal Highway Administration (FHWA 2015, 2-1 - 2-11). The bridge was modeled using the methods presented in Section 5. The live loading methods presented in this section were applied to the bridge model using both SAP2000 and CSiBridge and the LLDFs for each of the bridge models were calculated. These LLDFs were then compared with provided LLDFs calculated using the AASHTO BDS provisions.

6.5.1 Detail of Example Bridge

The bridge used to verify the live loading methods was a two-span, 220 ft. long continuously supported straight bridge with a cast-in-place concrete deck and six prestressed concrete underlying girders with intermediate diaphragms at the middle of each span (FHWA 2015, 2-1). The strength of the cast-in-place concrete deck was 4000 psi and the strength of the prestressed concrete girders was 6000 psi. Figure 6-27 presents an elevation view of the bridge. Figure 6-28 presents the transverse section of the bridge.

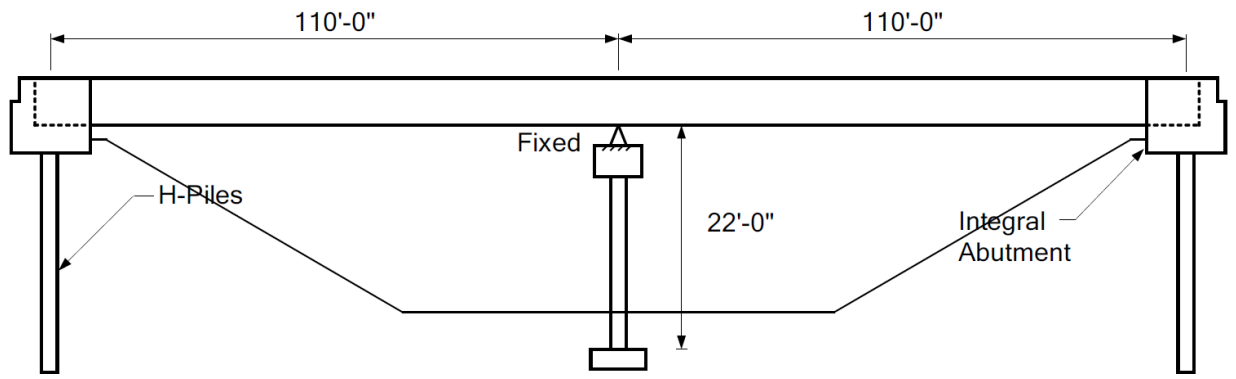


Figure 6-27: Elevation View of Example Bridge (FHWA 2015, 2-4)

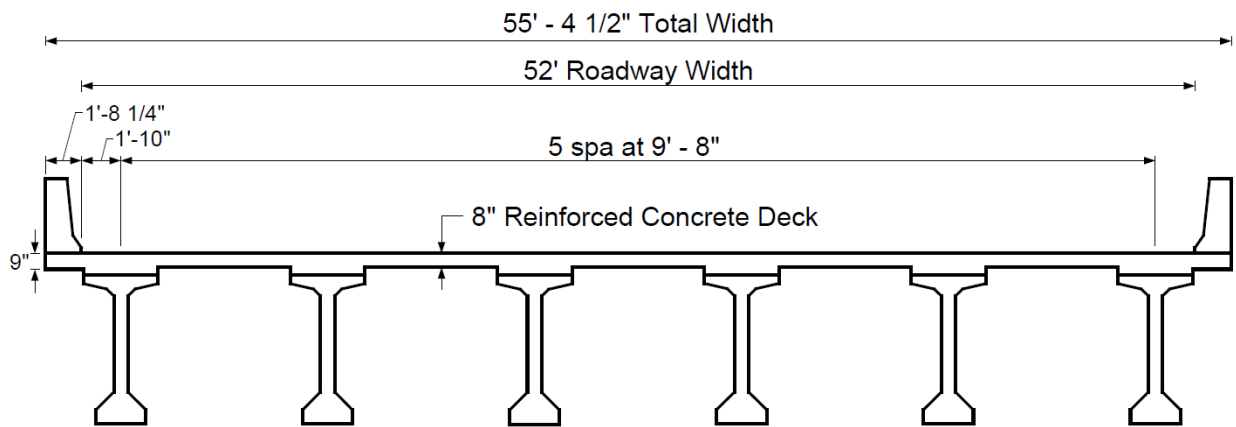


Figure 6-28: Transverse Section of Example Bridge (FHWA 2015, 2-4)

6.5.2 Comparison of Software LLDFs with AASHTO Hand-Calculated LLDFs

Using the developed modeling and live loading approach, a finite element model was created for the example bridge and live load analysis was conducted using SAP2000 and CSiBridge. Figure 6-29 presents the finite element model that was created for the example bridge.

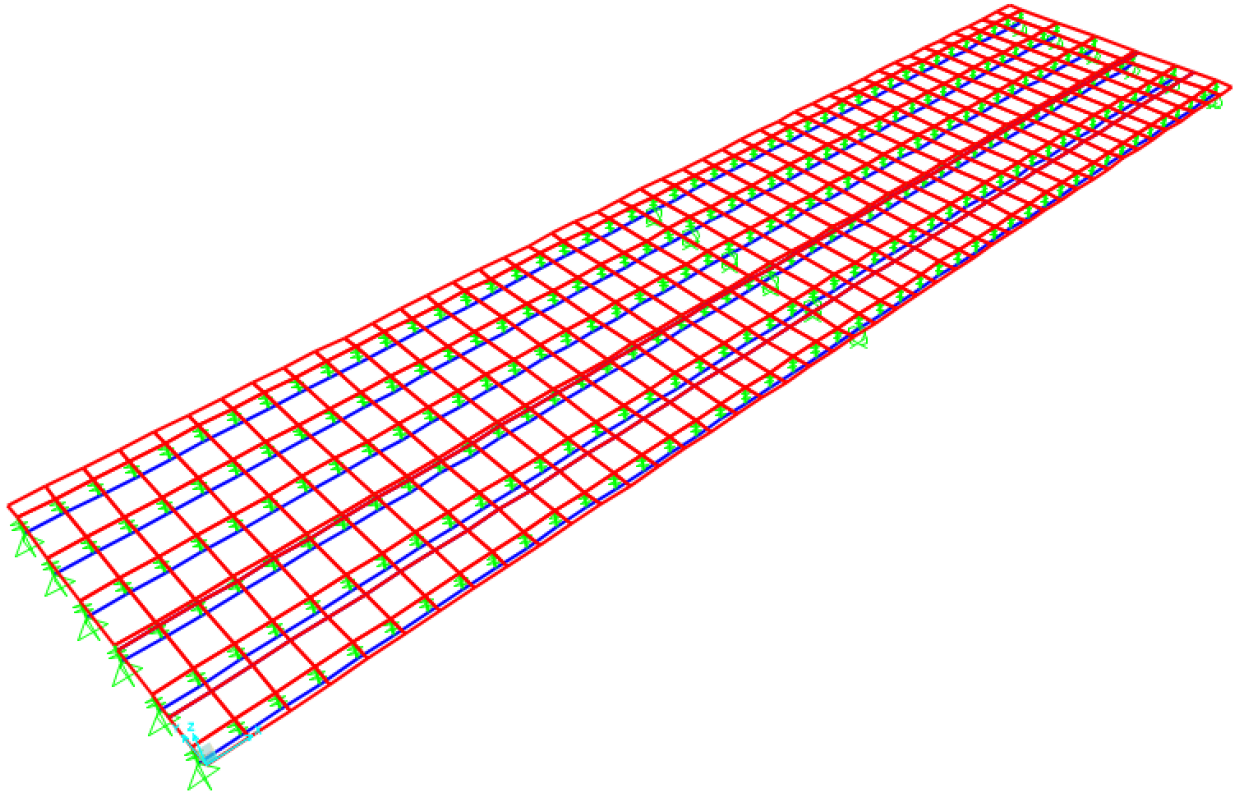


Figure 6-29: Finite Element Model of Example Bridge

From the finite element analysis conducted on the example bridge models, the controlling LLDFs were calculated for the positive moment and the negative moment. These controlling LLDFs were then compared to the LLDFs calculated by the FHWA using the AASHTO provisions. Table 6-8 presents the LLDFs calculated from SAP2000, CSiBridge, and the AASHTO LLDFs for positive and negative bending moments.

Table 6-8: LLDFs of Positive and Negative Bending Moments for the Example Bridge

	One Lane Loaded			Two Lanes Loaded		
	AASHTO Provisions	SAP2000	CSiBridge	AASHTO Provisions	SAP2000	CSiBridge
<i>Positive Bending Moments</i>						
Exterior Girders	0.81	0.53	0.55	0.77	0.60	0.65
Interior Girders	0.54	0.46	0.41	0.80	0.59	0.58
<i>Negative Bending Moments</i>						
Exterior Girders	0.81	0.53	0.55	0.77	0.60	0.65
Interior Girders	0.54	0.46	0.41	0.80	0.59	0.58

To analyze the difference between the software calculated LLDFs and the hand calculated LLDFs in the LLDFs, the percent error was calculated with the AASHTO hand calculated LLDFs as the known value control. The percent error was calculated as

$$\% \text{ Error} = \frac{LLDF_{AASHTO} - LLDF_{FEA}}{LLDF_{FEA}} * 100\%$$

where $LLDF_{AASHTO}$ is the hand calculated LLDF and $LLDF_{FEA}$ is the software calculated LLDF (NC State University n.d.). Table 6-9 compares the software calculated LLDFs and the AASHTO LLDFs for the positive bending moments and the negative bending moments.

Table 6-9: Comparison of Software Calculated & Provided LLDFs of Positive and Negative Bending Moments for the Example Bridge

	One Lane Loaded		Two Lanes Loaded	
	SAP2000	CSiBridge	SAP2000	CSiBridge
Positive Bending Moments				
Exterior Girders	34%	32%	22%	15%
Interior Girders	16%	25%	26%	28%
Negative Bending Moments				
Exterior Girders	32%	27%	22%	15%
Interior Girders	6%	17%	19%	21%

NOTE: Positive percentage indicates that AASHTO LLDF is larger than software calculated LLDF

As can be seen in the percent differences presented in Table 6-9, the LLDFs obtained from finite element analysis were smaller compared to the LLDFs calculated using the AASHTO provisions, making the AASHTO LLDFs more conservative. For the exterior girders, the difference in the LLDFs was as high as 34%. For the interior girders, the difference in the LLDFs was as high as 28%. For positive LLDFs, the average difference was 24% for LLDFs from SAP2000 and 25% for LLDFs from CSiBridge. For negative LLDFs, the average difference was 20% for LLDFs from both SAP2000 and CSiBridge.

These results match the previous findings of literature that, for straight bridges, LLDFs calculated using the AASHTO provisions are conservative compared to LLDFs calculated using finite element analysis or other types of refined analysis (Zaki 2016, 69). Research has found that the degree of conservatism of the AASHTO provisions varies greatly depending on the properties of the bridge such as the span-to-depth ratio and the presence of mid-span diaphragms (Barr, Eberhard and Stanton 2001, 305). Per the research conducted by Barr, Eberhard, and Stanton, LLDFs calculated using the AASHTO equations may be up to 28% higher than LLDFs obtained by finite element analysis (Barr, Eberhard and Stanton 2001, 305). Per the research

conducted by Chen & Aswad, the degree of conservatism for interior girder LLDFs ranged between 18-23% for interior girders and up to 30% for exterior girders when mid-span diaphragms are present (Chen and Aswad 1996, 120).

6.5.3 Comparison of SAP2000 & CSiBridge LLDFs for Example Bridge

The LLDFs for the example bridge that were obtained from the analyses conducted using both SAP2000 and CSiBridge were compared using percent difference. Percent difference was used instead of percent error since there is no control value between the SAP2000 and CSiBridge LLDFs. Percent difference was calculated as

$$\% \text{ Difference} = \frac{LLDF_{CSiBridge} - LLDF_{SAP2000}}{\frac{LLDF_{CSiBridge} + LLDF_{SAP2000}}{2}} * 100\%.$$

The percent differences of the controlling LLDFs are presented in Table 6-10.

Table 6-10: Comparison of SAP2000 & CSiBridge LLDFs of Positive and Negative Bending Moments for the Example Bridge

No. of Lanes Loaded	Positive LLDFs		Negative LLDFs	
	One Lane	Two Lanes	One Lane	Two Lanes
Exterior Girder	3%	8%	6%	9%
Interior Girders	-11%	-2%	-13%	-2%

NOTE: Positive percentage indicates that CSiBridge LLDF is larger than the SAP2000 LLDF.

Per the data presented in Table 6-10, there was a small difference in the LLDFs obtained through CSiBridge and those obtained through SAP2000. For the exterior girders, CSiBridge generated LLDFs up to 9% greater than those generated by SAP2000. For the interior girders, SAP2000 generated LLDFs up to 13% greater than CSiBridge.

An outlier case existed for the LLDFs generated by SAP2000 for the interior girders when one lane was loaded. This is the only case where the LLDFs generated by SAP2000 were significantly larger than those generated by CSiBridge. Additionally, the difference in LLDFs for

two lanes loaded was only 2%. This outlier can be attributed to how the two programs apply the vehicle load over the bridge.

As previously stated in Section 6.2, vehicles in SAP2000 can only be defined in the longitudinal direction (CSI 2016, 479-480). Therefore, two separate vehicle paths were required per lane to simulate the full force of the HL-93 load. While this solution allowed for the design trucks to be applied in full to the bridge, there were no options to get the program to recognize the two separate paths as acting together. This means that when SAP2000 was calculating the maximum forces due to the loaded vehicle paths, the load on one path may be at a different longitudinal position than the other path.

7 Results & Discussion

The results of the live loading conducted on the horizontally curved bridge models and the straight bridge models are presented in this section. Section 7.1 presents the controlling LLDFs for the bridge models for the analyses conducted with both SAP2000 and CSiBridge. Section 7.2 presents the difference between the LLDFs obtained from SAP2000 and those obtained from CSiBridge and a discussion of the results. Section 7.3 presents the difference between the horizontally curved bridge models and the straight bridge models and a discussion of the results. The full set of LLDFs calculated for each bridge model can be found in the appendix.

7.1 Controlling LLDFs

The controlling LLDFs for the four bridge models, one horizontally curved bridge model and one straight bridge model loaded using both SAP2000 and CSiBridge, are presented. The full set of LLDFs calculated for each bridge model can be found in the appendix.

7.1.1 Controlling LLDFs for Horizontally Curved Bridge

The controlling LLDFs for the horizontally curved bridge models loaded and analyzed in SAP2000 and CSiBridge are presented. The controlling LLDFs were calculated for one lane loaded, two lanes loaded, three lanes loaded, and all four lanes loaded. Table 7-11 presents the controlling LLDFs of positive and negative bending moments for the horizontally curved bridge obtained from SAP2000 and CSiBridge.

Table 7-11: LLDFs of Positive and Negative Bending Moments for the Horizontally Curved Bridge from SAP2000 and CSiBridge

<i>No. of Lanes Loaded</i>	<i>Positive LLDFs</i>				<i>Negative LLDFs</i>			
	One Lane	Two Lanes	Three Lanes	Four Lanes	One Lane	Two Lanes	Three Lanes	Four Lanes
SAP2000								
Exterior Girders	0.35	0.45	0.52	0.48	0.39	0.48	0.55	0.51
Interior Girders	0.28	0.40	0.48	0.46	0.30	0.41	0.50	0.49
CSiBridge								
Exterior Girders	0.38	0.51	0.53	0.43	0.44	0.56	0.55	0.42
Interior Girders	0.28	0.42	0.46	0.40	0.31	0.46	0.49	0.41

A visualization of the controlling LLDFs was created using column charts displaying the controlling exterior and interior LLDFs. For the LLDFs obtained using SAP2000, the controlling positive LLDFs are presented in Figure 7-30 and the controlling negative LLDFs are presented in Figure 7-31. For the LLDFs obtained using CSiBridge, the controlling positive LLDFs are presented in Figure 7-32 and the controlling negative LLDFs are presented in Figure 7-33.

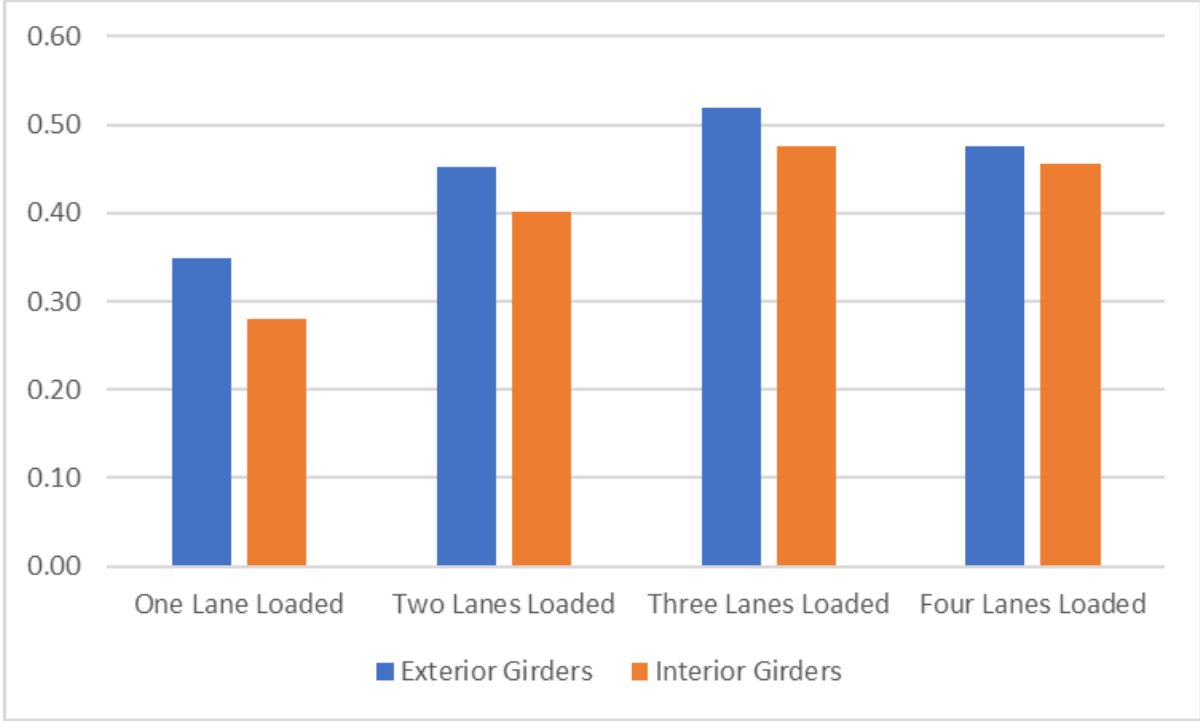


Figure 7-30: Positive LLDFs for Horizontally Curved Bridge from SAP2000

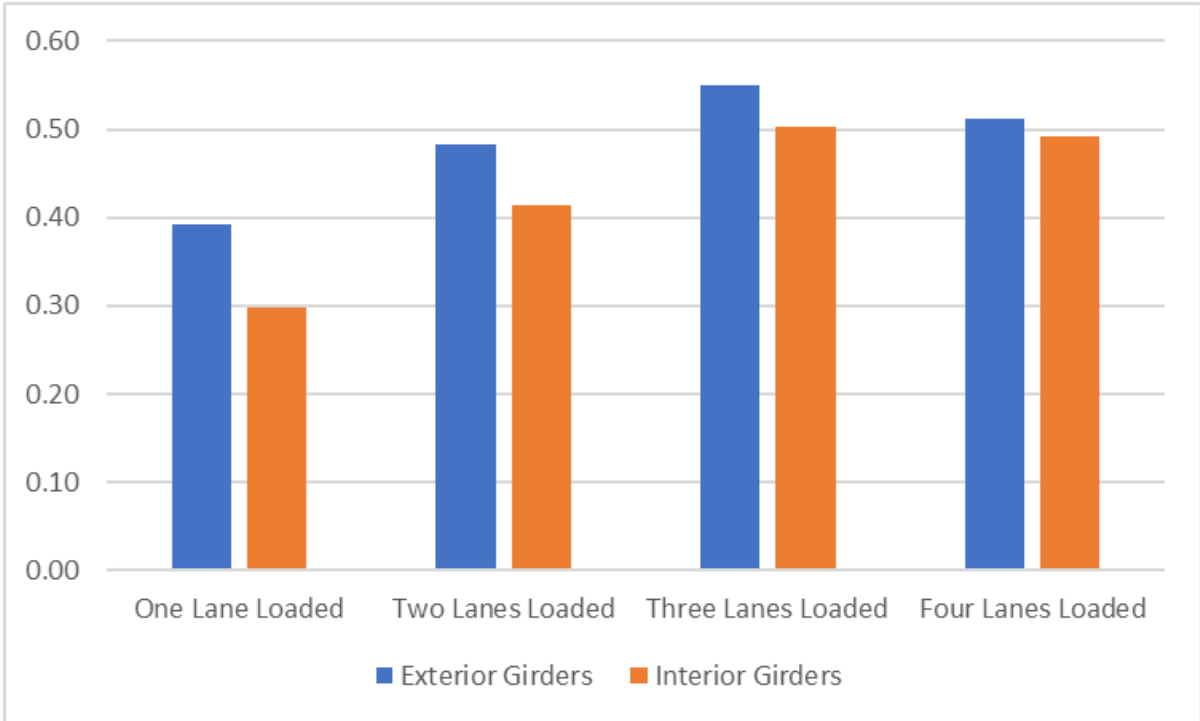


Figure 7-31: Negative LLDFs for Horizontally Curved Bridge from SAP2000

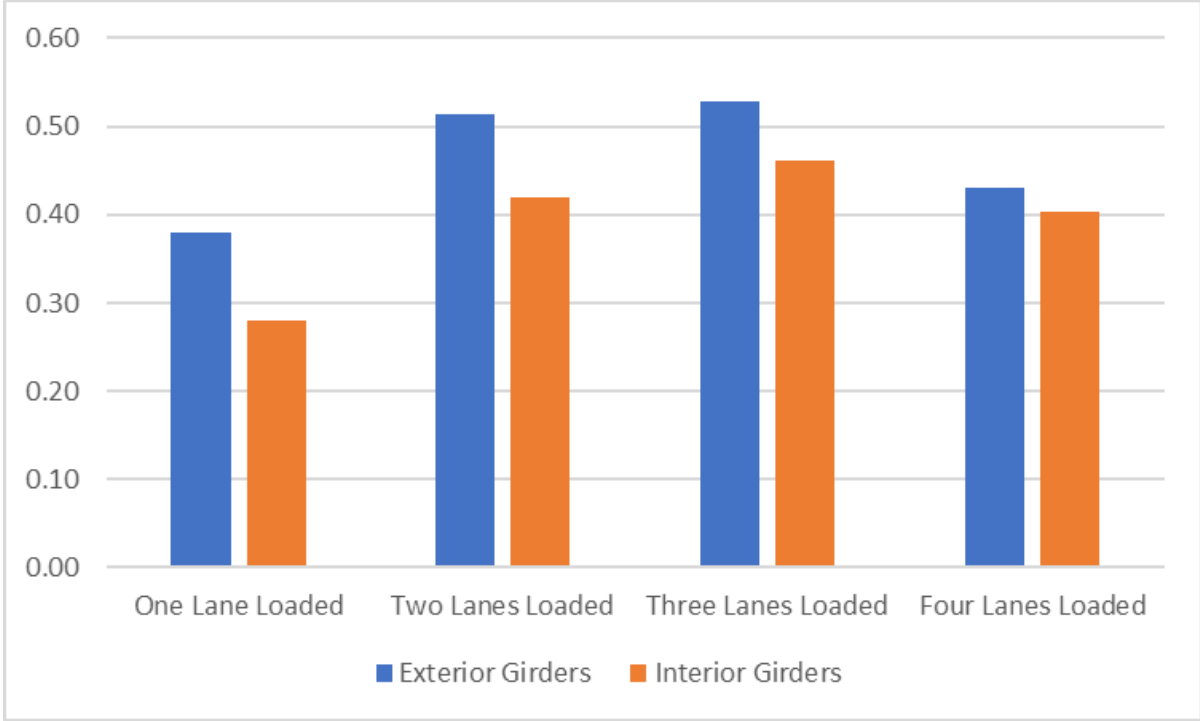


Figure 7-32: Positive LLDFs for Horizontally Curved Bridge from CSiBridge

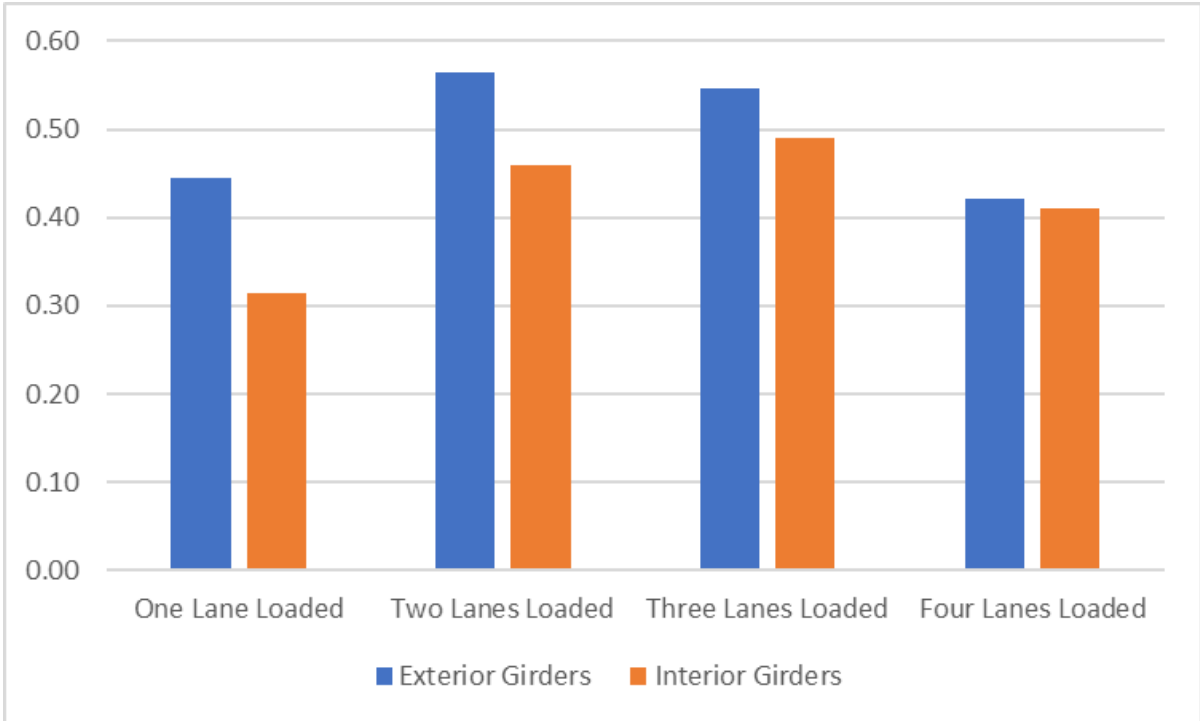


Figure 7-33: Negative LLDFs for Horizontally Curved Bridge from CSiBridge

7.1.2 Controlling LLDFs for Straight Bridge

The controlling LLDFs for the straight bridge models loaded and analyzed in SAP2000 and CSiBridge are presented. The controlling LLDFs were calculated for one lane loaded, two lanes loaded, three lanes loaded, and all four lanes loaded. Table 7-12 presents the controlling LLDFs of positive and negative bending moments for the straight bridge obtained from SAP2000 and CSiBridge.

Table 7-12: LLDFs of Positive and Negative Bending Moments for the Straight Bridge from SAP2000 and CSiBridge

<i>No. of Lanes Loaded</i>	<i>Positive LLDFs</i>				<i>Negative LLDFs</i>			
	One Lane	Two Lanes	Three Lanes	Four Lanes	One Lane	Two Lanes	Three Lanes	Four Lanes
<i>SAP2000</i>								
Exterior Girders	0.34	0.48	0.51	0.60	0.40	0.52	0.54	0.60
Interior Girders	0.25	0.39	0.44	0.58	0.29	0.45	0.50	0.59
<i>CSiBridge</i>								
Exterior Girders	0.35	0.48	0.49	0.40	0.42	0.55	0.54	0.42
Interior Girders	0.27	0.40	0.44	0.39	0.31	0.45	0.49	0.40

A visualization of the controlling LLDFs was created using column charts displaying the controlling exterior and interior LLDFs. For the LLDFs obtained using SAP2000, the controlling positive LLDFs are presented in Figure 7-34 and the controlling negative LLDFs are presented in Figure 7-35. For the LLDFs obtained using CSiBridge, the controlling positive LLDFs are presented in Figure 7-36 and the controlling negative LLDFs are presented in Figure 7-37.

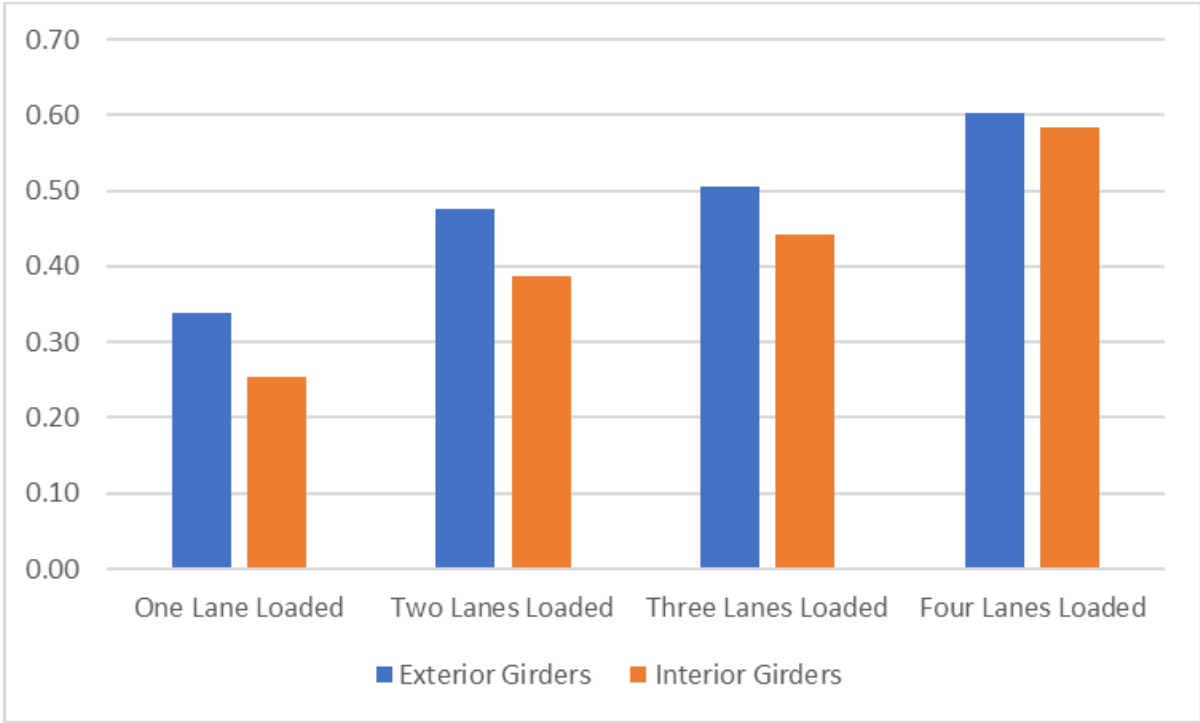


Figure 7-34: Positive LLDFs for Straight Bridge from SAP2000

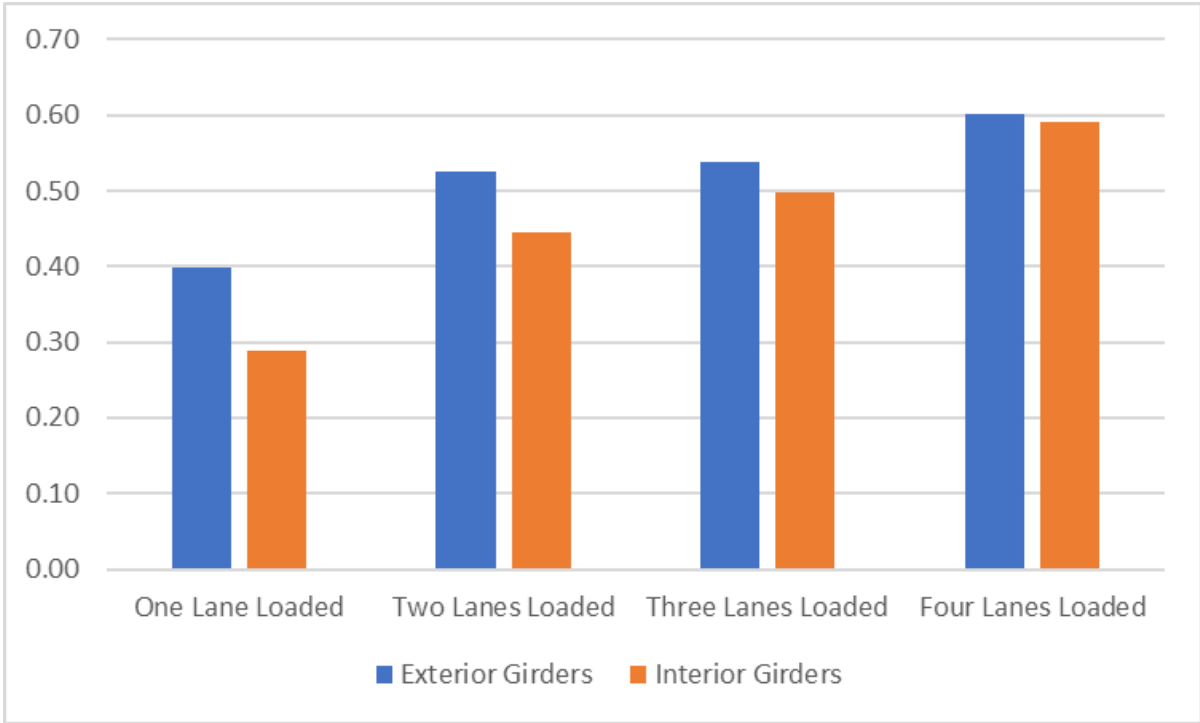


Figure 7-35: Negative LLDFs for Straight Bridge from SAP2000

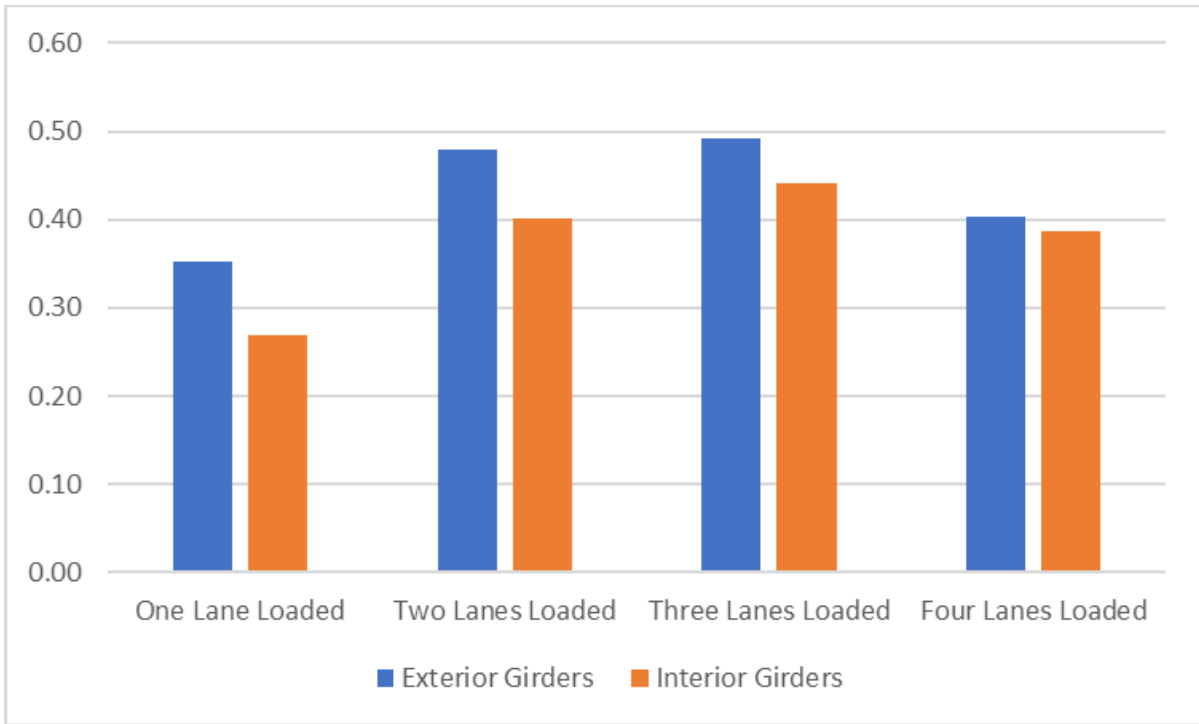


Figure 7-36: Positive LLDFs for Straight Bridge from CSiBridge

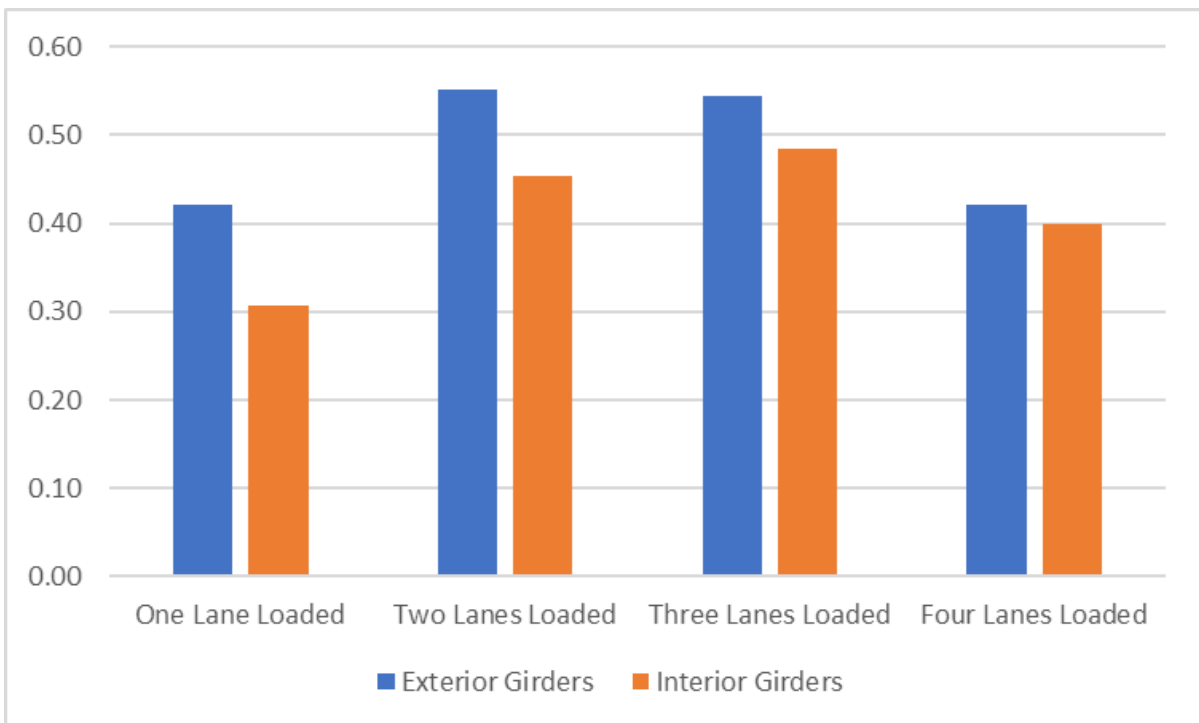


Figure 7-37: Negative LLDFs for Straight Bridge from CSiBridge

7.2 Comparison of LLDFs Calculated with SAP2000 & CSiBridge

The LLDFs for the horizontally curved bridge and the straight bridge calculated with SAP2000 and CSiBridge were compared with percent difference to observe the difference between the two programs using the percent difference equation presented in Section 6.4. The comparison of LLDFs is presented in Table 7-13 for the horizontally curved bridge and for the straight bridge.

Table 7-13: Comparison of SAP2000 & CSiBridge LLDFs for Horizontally Curved Bridge & Straight Bridge

<i>No. of Lanes Loaded</i>	<i>Positive LLDFs</i>				<i>Negative LLDFs</i>			
	One Lane	Two Lanes	Three Lanes	Four Lanes	One Lane	Two Lanes	Three Lanes	Four Lanes
<i>Horizontally Curved Bridge</i>								
Exterior Girders	8%	13%	2%	-10%	13%	16%	-1%	-20%
Interior Girders	0%	4%	-3%	-12%	6%	10%	-3%	-18%
<i>Straight Bridge</i>								
Exterior Girders	4%	1%	-3%	-39%	6%	5%	1%	-35%
Interior Girders	6%	3%	0%	-41%	6%	2%	-2%	-39%

NOTE: Positive percentage indicates that CSiBridge LLDF is larger than the SAP2000 LLDF.

A difference was observed in the LLDFs calculated with SAP2000 compared to LLDFs calculated with CSiBridge. As can be seen in Table 7-13, the degree of difference between the LLDFs ranged from marginal (0% - 3%) to extreme (35% - 41%). From these data, trends were observed.

For both the horizontally curved bridge and straight bridge, the controlling LLDFs generated by CSiBridge were typically larger than those generated by SAP2000. The difference in LLDFs was slightly greater for exterior girders compared to interior girders on average. The difference

between negative LLDFs were slightly more pronounced than for positive LLDFs on average. Additionally, the difference in LLDFs was greater between the programs for the curved bridge models compared to the straight bridge models.

For the straight bridge there was a significant difference between the LLDFs for all lanes loaded. For this case, the LLDFs generated by SAP2000 ranged from 35% - 41% larger than those generated by CSiBridge. This difference was observed for both the positive LLDFs and the negative LLDFs. These data are exceptional since the differences in LLDFs for the other load cases were significantly smaller, with an average of 2% in favor of CSiBridge.

Similar outliers were observed for the horizontally curved bridge. For all lanes loaded, the LLDFs generated by SAP2000 were significantly greater than those generated by CSiBridge by up to 18%. For all other load cases, the LLDFs were greater for CSiBridge or very slightly larger for SAP2000. However, the degree of the difference for these outliers are less extreme than the LLDFs for the straight bridge.

These outliers can be explained by the difference in moving load functionality between SAP2000 and CSiBridge. To properly apply the AASHTO design truck to the bridge models in SAP2000, separate vehicle paths were required for each half of the truck, as detailed in Section 6.2. To simulate the full design truck, moving load cases were made which applied the defined vehicular loads to the two paths. Despite the lanes being loaded together, SAP2000 still viewed these paths as two distinctly loaded lanes. When calculating the maximum force envelopes, error could be propagated since there is no way for the program to recognize the two separate paths as one vehicle which is restrained to one longitudinal position at a time.

Additional errors were propagated due to the limitations on the transverse movement of vehicles in SAP2000. Since the program does not allow lane widths to be assigned to defined paths, vehicle loads applied to the paths cannot be moved transversely (CSI 2016, 479-480). This resulted in decreased accuracy of the SAP2000 LLDFs since the HL-93 design trucks could not be moved transversely to better calculate the maximum force envelope (Zaki 2016, 26). However, even if this functionality were provided, it would not be of use for the live loading conducted since the vehicle loads would need to be held at a constant 6 ft. width. Additional

functionality would be required to join the two vehicle paths together in both the longitudinal and transverse directions to increase the accuracy of the live loading.

From these findings it was concluded that CSiBridge provides a higher degree of accuracy for applying vehicular live load and calculating LLDFs compared to SAP2000. Compared to SAP2000, CSiBridge allows for vehicles to be fully loaded onto a defined lane and moved transversely along the width of the lane to better calculate the maximum forces (Zaki 2016, 26). This is reflected in the comparisons made between the LLDFs from the bridges analyzed with SAP2000 and the bridges analyzed with CSiBridge (Table 7-13). From these comparisons it was observed that the LLDFs from CSiBridge were more conservative than the LLDFs from SAP2000, with the exceptions of the outliers that were previously discussed. Additionally, the makers of SAP2000 and CSiBridge, Computers & Structures, Inc. recommend that CSiBridge be used for vehicular loading of bridges and advanced bridge analysis (CSI 2016, 478-479). The results of this study concur with this recommendation.

7.3 Comparison of Horizontally Curved Bridge & Straight Bridge LLDFs

The LLDFs for the horizontally curved bridge and the straight bridge were compared using percent difference to observe the effects of curvature on LLDFs using the percent difference equation presented in Section 6.4. To adequately judge the effects of curvature, separate comparisons were made between the LLDFs calculated with SAP2000 and the LLDFs calculated with CSiBridge. The comparison of LLDFs from the SAP2000 models and the CSiBridge models is presented in Table 7-14.

Table 7-14: Comparison of SAP2000 & CSiBridge LLDFs for Horizontally Curved Bridge & Straight Bridge

<i>No. of Lanes Loaded</i>	<i>Positive LLDFs</i>				<i>Negative LLDFs</i>			
	One Lane	Two Lanes	Three Lanes	Four Lanes	One Lane	Two Lanes	Three Lanes	Four Lanes
SAP2000								
Exterior Girders	3%	-5%	2%	-23%	-2%	-8%	2%	-16%
Interior Girders	10%	4%	8%	-25%	3%	-7%	1%	-18%
CSiBridge								
Exterior Girders	7%	7%	7%	6%	5%	3%	0%	0%
Interior Girders	4%	4%	4%	4%	2%	1%	1%	2%

NOTE: Positive percentage indicates that horizontally curved bridge LLDF is larger than the straight bridge LLDF.

The LLDFs of the horizontally curved bridge models and the straight bridge models were compared to analyze the effects of curvature on LLDFs. The bridge models analyzed using SAP2000 and the bridge models analyzed using CSiBridge (Table 7-14) were compared. From prior research it is known that curvature is responsible for increases in the maximum forces experienced by bridges (Khakafalla and Sennah 2014, 13). As a result, LLDFs will increase when horizontal curvature is introduced to a bridge (Zaki 2016, 70).

Since the results from SAP2000 were not conclusive, the difference in LLDFs for the horizontally curved bridge and straight bridge from the CSiBridge models were compared to investigate the effects of curvature. The percent differences between the curved bridge and straight bridge LLDFs are presented in Table 7-14. As can be seen, the LLDFs are larger for the horizontally curved bridge than for the straight bridge which concur with the expected results

from literature. There were no cases where the LLDFs from the straight bridge were larger than for the curved bridge.

Observations were made from the differences in the LLDFs between the horizontally curved bridge and the straight bridge. It was observed that the difference due to curvature was greater for the positive LLDFs than for the negative LLDFs. For positive LLDFs, the difference varied from 4% - 7%. For negative LLDFs, the difference varied from 0%, meaning that there was no difference between the curved bridge and straight bridge LLDFs, to 5%. Per the research conducted by Zaki, the differences between the maximum negative LLDFs and LLDFs calculated using the AASHTO provisions were smaller than for the positive moment (Zaki 2016, 34). However, comparisons were not made between the positive and negative LLDFs. Additional research is required to further investigate the degree of difference between positive and negative LLDFs due to curvature.

It was observed that the difference in LLDFs due to curvature was more pronounced for exterior girders compared to interior girders. For the positive LLDFs, the difference in LLDFs for exterior girders was 3 to 4 percentage points greater than the difference in LLDFs for interior girders. Literature states that the LLDFs obtained from finite element analysis for exterior girders are generally larger than the LLDFs for interior girders (Chen and Aswad 1996, 120). This can be seen in the LLDFs for the bridge models visualized in Figure 7-32, Figure 7-33, Figure 7-36, and Figure 7-37 where the LLDFs for all load cases were larger for exterior girders than for interior girders. As previously stated, the introduction of curvature results in an increase of the structural response of the bridge and an increase in LLDFs (Khakafalla and Sennah 2014, 13) (Zaki 2016, 70). Since the LLDFs for exterior girders are larger to begin with, it follows that an increase in curvature would illicit a greater change in the structural response of these members when compared to interior girders.

Lastly, it was observed that the difference in LLDFs due to curvature was not impacted by the number of lanes loaded for positive LLDFs. As can be seen in Table 7-14, the differences in LLDFs for positive LLDFs for one lane loaded, two lanes loaded, three lanes loaded, and four lanes loaded were negligible. However, for negative LLDFs, the difference due to curvature

decreased as more lanes were loaded. Additional research is required to further investigate these findings.

8 Conclusions & Future Research

An approach was developed to calculate LLDFs for horizontally curved bridges with underlying straight girders using generalized finite element tools with geometrical simplifications in models. This approach was verified using an example bridge designed by the FHWA with existing LLDF calculations per AASHTO BDS (FHWA 2015, 2-1 - 2-11) and was then applied to one straight bridge and one curved bridge model, both based on an existing highway bridge in the state of Pennsylvania. Using the LLDFs calculated from SAP2000 and CSiBridge for these models, conclusions were made regarding the accuracy of the loading procedures implemented by each software package and the effects of curvature on the LLDFs for horizontally curved bridges with straight underlying girders.

From the analysis conducted, the following conclusions and observations were made:

1. To calculate accurate LLDFs, CSiBridge is recommended over SAP2000 due to the presence of greater functionality for applying vehicle live load to bridge models.
2. The LLDFs for positive moment were impacted more by the effects of horizontal curvature than the LLDFs for negative moment.
3. Horizontal curvature causes a greater increase in LLDFs for exterior girders compared to interior girders.

Further research is recommended to validate and expand upon the observations and conclusions made from the results of this study. As presented in Table 7-14, the effects of curvature presented themselves differently for positive LLDFs and for negative LLDFs. Applying the developed approach to additional bridges of varying curvature would provide a larger sample of data that could be analyzed to further investigate these differences and draw conclusions. Also, the effects of curvature on exterior and interior girders could be investigated further with more bridge data.

It is recommended that the accuracy of the AASHTO LLDF equations in Article 4.6.2.2 for horizontally curved bridges with straight bridges be investigated. Using the developed approach, LLDFs for bridges of varying curvature using finite element analysis could be compared to

LLDFs calculated using the AASHTO equations. It would be of use to engineers if a range of applicability for the AASHTO LLDF equations could be defined. Additionally, the development of curvature correction factors or a mathematic relationship for the AASHTO LLDF equations would help to increase the range of applicability of the current AASHTO provisions.

Additionally, the modeling techniques developed as part of this study should be further refined. Advanced modeling techniques or developments in modeling technology should be investigated and incorporated into the developed modeling approach to increase the speed at which users can create finite element models and to increase the accuracy of the models.

References

- AASHTO. 2012. "AASHTO LRFD Bridge Design Specifications." Washington, DC: AASHTO. 3-i - 4-74.
- Amorn, Wilast, Christopher Y. Tuan, and Maher K. Tadros. 2008. "Curved, precast, pretensioned concrete I-girder bridges." *PCI Journal* 53 (6): 48-66.
- Autodesk. 2020. "AutoCAD LT." San Rafael, CA: Autodesk, Inc.
- Barr, Paul J, Marc O Eberhard, and John F Stanton. 2001. "Live Load Distribution Factors in Prestressed Concrete Girders." *Journal of Bridge Engineering* 298-306.
- Chen, Yochida, and Alex Aswad. 1996. "Stretching Span Capability of Prestressed Concrete Bridges Under AASHTO LRFD." *Journal of Bridge Engineering* 1 (3): 112-120.
- CSI. 2016. *CSI Analysis Reference Manual*. 19. Berkeley, CA: Computers & Structures, Inc.
- . 2022. "CSiBridge." Walnut Creek, CA: Computers & Structures, Inc.
- . 2004. "Linear and Nonlinear Static and Dynamic Analysis of Three Dimensional Structures - Getting Started." Berkeley, CA.
- . 2016. "SAP2000." Walnut Creek, CA: Computers & Structures, Inc.
- FHWA. 2015. "Load and Resistance Factor Design (LRFD) for Highway Bridge Superstructure Reference Manual." Arlington, Virginia.
- FHWA. 2015. *Load and Resistance Factor Design (LRFD) for Highway Bridge Superstructures Design Examples*. U.S. Department of Transportation.
- Google Maps. n.d. *US-15 Highway Bridge Lawrenceville, PA*. Accessed August 28, 2022. maps.google.com.
- Khakafalla, Imad Eldin, and Khaled Sennah. 2014. "Curvature Limitations for Slab-on-I-Girder Bridges." *Journal of Bridge Engineering* (American Society of Civil Engineers) 19 (9).
- Lewis, Myles E.H. 2016. "Kinked Straight Girders Forming Horizontally Curved Alignments on Northeast Anthony Henday Drive." Calgary, AL, Canada.
- Mannering, Fred L., and Scott S. Washburn. 2013. *Principles of Highway Engineering and Traffic Analysis*. 5th. John Wiley & Sons, Inc.

- Mensah, Salahudin A. 2006. "Live Load Distribution Factors in Two-Girder Bridge Systems Using Precast Trapezoidal U-Girders." M.S. Thesis, Univ. of Colorado, Denver, Denver, CO.
- NC State University. n.d. "Percent Error and Percent Difference." *Mechanics Third Edition - NC State University Physics Department*. Accessed November 29, 2022. https://www.webassign.net/question_assets/ncsucalcphysmechl3/percent_error/manual.html.
- Nowak, Michael D. 2018. *Mechanics of Material Laboratory Manual*. 3.5. Hartford, CT.
- PennDOT. 2019. *Concrete Field Testing Technician Certification Field Manual*. 2019 Edition. Harrisburg, PA: PennDOT.
- . 2005. "S.R. 6015 (SB) Sec. 22E Over Cowanesque River & Proposed S.R. 4022 6 Span Cont Comp P/C Conc I-Beam Bridge." November 17.
- Sotelino, Elisa D., Judy Liu, Wonseok Chung, and Kitjapat Phuvoravan. 2004. *Simplified Load Distribution Factor for Use In LRFD Design*. School of Civil Engineering, Purdue University, West Lafayette: U.S. Federal Highway Administration, 203.
- Wolfram. n.d. "Parabolic Segment." *Wolfram Mathworld*. <https://mathworld.wolfram.com/ParabolicSegment.html>.
- Yousif, Zaher, and Riyadh Hindi. 2006. "Live Load Distribution Factor for Highway Bridges Based on AASHTO-LRFD and Finite Element Analysis." *Structures Congress 2006* (American Society of Civil Engineers).
- Zaki, Mohammed. 2016. "Live Load Distribution Factors for Horizontally Curved Concrete Box Girder Bridges." M.S. thesis, Dept. Civil and Env. Eng., Univ. Massachusetts Amherst, Amherst, MA.

9 Appendix

Table 9-15: LLDFs of Positive and Negative Bending Moments for the Horizontally Curved Bridge from SAP2000

DISTRIBUTION FACTORS - POSITIVE MOMENT															
	COMB1	COMB2	COMB3	COMB4	COMB5	COMB6	COMB7	COMB8	COMB9	COMB10	COMB11	COMB12	COMB13	COMB14	COMB15
Girder 1	0.35	0.18	0.15	0.06	0.45	0.44	0.35	0.29	0.21	0.19	0.52	0.45	0.44	0.31	0.48
Girder 2	0.28	0.19	0.16	0.09	0.40	0.38	0.32	0.30	0.24	0.22	0.48	0.43	0.41	0.34	0.46
Girder 3	0.20	0.20	0.17	0.13	0.34	0.32	0.29	0.32	0.29	0.26	0.43	0.40	0.39	0.38	0.44
Girder 4	0.14	0.18	0.19	0.18	0.27	0.28	0.27	0.32	0.31	0.32	0.38	0.38	0.39	0.41	0.35
Girder 5	0.08	0.15	0.19	0.25	0.21	0.23	0.28	0.30	0.34	0.37	0.32	0.37	0.38	0.44	0.41
Girder 6	0.03	0.14	0.18	0.32	0.16	0.18	0.30	0.27	0.39	0.42	0.27	0.37	0.38	0.47	0.40
DISTRIBUTION FACTORS - NEGATIVE MOMENT															
	COMB1	COMB2	COMB3	COMB4	COMB5	COMB6	COMB7	COMB8	COMB9	COMB10	COMB11	COMB12	COMB13	COMB14	COMB15
Girder 1	0.39	0.16	0.15	0.05	0.47	0.48	0.39	0.27	0.18	0.19	0.55	0.46	0.49	0.30	0.51
Girder 2	0.30	0.18	0.16	0.08	0.41	0.41	0.34	0.30	0.23	0.23	0.50	0.44	0.44	0.34	0.49
Girder 3	0.20	0.20	0.17	0.13	0.34	0.33	0.30	0.32	0.29	0.27	0.44	0.42	0.40	0.40	0.47
Girder 4	0.12	0.19	0.19	0.19	0.27	0.26	0.27	0.32	0.33	0.32	0.38	0.38	0.38	0.43	0.44
Girder 5	0.05	0.17	0.18	0.26	0.20	0.20	0.27	0.31	0.37	0.37	0.31	0.37	0.36	0.46	0.42
Girder 6	0.03	0.13	0.16	0.34	0.13	0.14	0.29	0.25	0.41	0.42	0.23	0.36	0.36	0.47	0.38

Table 9-16: LLDFs of Positive and Negative Bending Moments for the Straight Bridge from SAP2000

DISTRIBUTION FACTORS - POSITIVE MOMENT															
	COMB1	COMB2	COMB3	COMB4	COMB5	COMB6	COMB7	COMB8	COMB9	COMB10	COMB11	COMB12	COMB13	COMB14	COMB15
Girder 1	0.30	0.19	0.14	0.07	0.41	0.35	0.29	0.28	0.22	0.18	0.46	0.40	0.34	0.30	0.55
Girder 2	0.23	0.19	0.14	0.09	0.37	0.32	0.27	0.28	0.24	0.19	0.43	0.39	0.35	0.32	0.56
Girder 3	0.20	0.19	0.15	0.13	0.33	0.30	0.27	0.30	0.28	0.24	0.40	0.38	0.35	0.36	0.57
Girder 4	0.17	0.16	0.19	0.18	0.28	0.29	0.29	0.30	0.29	0.32	0.37	0.37	0.39	0.40	0.57
Girder 5	0.11	0.14	0.20	0.25	0.21	0.25	0.30	0.28	0.33	0.39	0.32	0.37	0.41	0.44	0.58
Girder 6	0.06	0.12	0.21	0.34	0.15	0.21	0.33	0.28	0.39	0.48	0.28	0.38	0.44	0.51	0.60
DISTRIBUTION FACTORS - NEGATIVE MOMENT															
	COMB1	COMB2	COMB3	COMB4	COMB5	COMB6	COMB7	COMB8	COMB9	COMB10	COMB11	COMB12	COMB13	COMB14	COMB15
Girder 1	0.38	0.22	0.10	0.06	0.52	0.41	0.33	0.27	0.19	0.09	0.54	0.46	0.36	0.24	0.60
Girder 2	0.29	0.22	0.13	0.06	0.45	0.36	0.29	0.30	0.23	0.15	0.50	0.43	0.36	0.30	0.59
Girder 3	0.20	0.21	0.16	0.10	0.36	0.32	0.27	0.32	0.27	0.23	0.45	0.40	0.36	0.37	0.59
Girder 4	0.13	0.17	0.20	0.18	0.26	0.29	0.27	0.32	0.30	0.33	0.39	0.37	0.39	0.42	0.59
Girder 5	0.06	0.12	0.21	0.28	0.16	0.23	0.30	0.29	0.35	0.42	0.30	0.36	0.42	0.47	0.58
Girder 6	0.07	0.07	0.20	0.40	0.11	0.17	0.34	0.23	0.41	0.52	0.20	0.36	0.46	0.52	0.58

Table 9-17: LLDFs of Positive and Negative Bending Moments for the Horizontally Curved Bridge from CSiBridge

DISTRIBUTION FACTORS - POSITIVE MOMENT															
	COMB1	COMB2	COMB3	COMB4	COMB5	COMB6	COMB7	COMB8	COMB9	COMB10	COMB11	COMB12	COMB13	COMB14	COMB15
Girder 1	0.33	0.20	0.14	0.07	0.44	0.37	0.30	0.28	0.22	0.18	0.46	0.40	0.34	0.29	0.37
Girder 2	0.25	0.21	0.14	0.08	0.38	0.33	0.28	0.29	0.24	0.19	0.42	0.38	0.34	0.31	0.37
Girder 3	0.21	0.20	0.17	0.13	0.33	0.30	0.27	0.31	0.28	0.25	0.40	0.37	0.35	0.35	0.38
Girder 4	0.17	0.18	0.20	0.20	0.28	0.29	0.28	0.32	0.31	0.33	0.37	0.36	0.38	0.41	0.39
Girder 5	0.11	0.15	0.22	0.28	0.21	0.27	0.31	0.31	0.36	0.42	0.33	0.37	0.42	0.46	0.40
Girder 6	0.06	0.13	0.24	0.38	0.16	0.24	0.36	0.31	0.42	0.51	0.29	0.40	0.47	0.53	0.43
DISTRIBUTION FACTORS - NEGATIVE MOMENT															
	COMB1	COMB2	COMB3	COMB4	COMB5	COMB6	COMB7	COMB8	COMB9	COMB10	COMB11	COMB12	COMB13	COMB14	COMB15
Girder 1	0.33	0.19	0.08	0.06	0.43	0.34	0.28	0.23	0.16	0.09	0.43	0.37	0.30	0.19	0.33
Girder 2	0.24	0.18	0.11	0.06	0.35	0.29	0.23	0.24	0.19	0.12	0.38	0.33	0.28	0.24	0.31
Girder 3	0.16	0.17	0.14	0.09	0.28	0.25	0.21	0.26	0.22	0.19	0.33	0.30	0.28	0.28	0.30
Girder 4	0.10	0.14	0.17	0.16	0.20	0.22	0.22	0.26	0.25	0.27	0.29	0.28	0.30	0.33	0.31
Girder 5	0.06	0.11	0.18	0.25	0.13	0.20	0.25	0.25	0.30	0.36	0.25	0.29	0.34	0.38	0.32
Girder 6	0.06	0.08	0.18	0.35	0.11	0.16	0.30	0.21	0.35	0.44	0.18	0.30	0.38	0.43	0.33

Table 9-18: LLDFs of Positive and Negative Bending Moments for the Straight Bridge from CSiBridge

DISTRIBUTION FACTORS - POSITIVE MOMENT															
	COMB1	COMB2	COMB3	COMB4	COMB5	COMB6	COMB7	COMB8	COMB9	COMB10	COMB11	COMB12	COMB13	COMB14	COMB15
Girder 1	0.33	0.20	0.14	0.08	0.44	0.37	0.31	0.28	0.22	0.18	0.46	0.41	0.35	0.29	0.38
Girder 2	0.25	0.21	0.14	0.09	0.38	0.32	0.28	0.29	0.25	0.19	0.42	0.38	0.34	0.31	0.37
Girder 3	0.20	0.20	0.17	0.13	0.33	0.30	0.27	0.31	0.28	0.25	0.39	0.37	0.35	0.35	0.37
Girder 4	0.17	0.17	0.20	0.19	0.27	0.28	0.28	0.31	0.30	0.33	0.36	0.35	0.37	0.40	0.38
Girder 5	0.11	0.14	0.21	0.27	0.21	0.25	0.30	0.29	0.34	0.40	0.32	0.36	0.41	0.44	0.39
Girder 6	0.06	0.12	0.22	0.35	0.15	0.23	0.34	0.29	0.40	0.48	0.28	0.38	0.44	0.49	0.40
DISTRIBUTION FACTORS - NEGATIVE MOMENT															
	COMB1	COMB2	COMB3	COMB4	COMB5	COMB6	COMB7	COMB8	COMB9	COMB10	COMB11	COMB12	COMB13	COMB14	COMB15
Girder 1	0.33	0.19	0.08	0.06	0.43	0.34	0.28	0.23	0.16	0.09	0.43	0.37	0.30	0.20	0.33
Girder 2	0.24	0.19	0.11	0.06	0.35	0.29	0.23	0.25	0.19	0.13	0.38	0.33	0.28	0.24	0.31
Girder 3	0.16	0.17	0.14	0.09	0.28	0.25	0.21	0.25	0.21	0.19	0.33	0.30	0.28	0.28	0.30
Girder 4	0.10	0.14	0.16	0.15	0.20	0.22	0.21	0.25	0.24	0.26	0.28	0.28	0.29	0.32	0.30
Girder 5	0.06	0.11	0.17	0.23	0.13	0.19	0.23	0.23	0.28	0.34	0.23	0.27	0.32	0.36	0.30
Girder 6	0.06	0.07	0.17	0.33	0.11	0.15	0.28	0.20	0.33	0.42	0.17	0.28	0.36	0.40	0.31